5-2020

Dewatering of Chlorella Through Carbon Dioxide Hydrate Formation for Biofuel Production

Charles Dow

THE UNIVERSITY OF NEW HAVEN

DEWATERING OF *CHLORELLA* THROUGH CARBON DIOXIDE HYDRATE FORMATION FOR BIOFUEL PRODUCTION

A Thesis

submitted in partial fulfillment

of the requirements for the degree of

MASTER OF SCIENCE IN ENVIRONMENTAL ENGINEERING

BY

Charles Dow

University of New Haven

West Haven, Connecticut

May 2020

DEWATERING OF *CHLORELLA* THROUGH CARBON DIOXIDE HYDRATE FORMATION FOR BIOFUEL PRODUCTION

APPROVED BY

[Kristine Horvat, Ph.D.]
Thesis Adviser

[Emese Hadnagy, Ph.D.]
Committee Member

[Eddie Luzik, Ph.D.]
Committee Member

[Agamemnon Koutsospyros, Ph.D.]
Program Coordinator

[Ronald S. Harichandran, Ph.D.]
Dean of the College

[Mario T. Gaboury, J.D., Ph.D.]
Provost

ACKNOWLEDGMENTS

I would like to give special thanks to my thesis advisor Dr. Kristine Horvat. Her guidance and support through my master's program and thesis helped greatly in the completion of both. Thanks to her I have gained new experience and knowledge that will help me be prepared for employment and future endeavors.

I would like to thank Dr. Emese Hadnagy and Dr. Eddie Luzik for being part of my thesis committee.

I would like to thank Dr. Agamemnon Koutsospyros for leading the Master of Science Environmental Engineering program and aid in completing my thesis.

I would like to thank Stacie Merulo for their prior research with Dr. Kristine Horvat. This research provided carbon dioxide hydrate data for water and a methodology of calculating the water uptake by carbon dioxide hydrates.

I would like to thank Danielle Belskis for their prior research with Dr. Kristine Horvat. This research provided algae used in this study and determined algae that are grown in wastewater would not be able to be used in this study.

I would like to thank Michele Berman and Dino Dimas for their support and aid in maintaining safety and laboratory spaces.

I would like to thank Caroline Beech for their support through this entire process and someone I can bounce ideas off of.

I would like to thank Denise and Chuck Dow for ultimately convincing me to pursue my master's degree.

I would like to thank Jorge Perez, Efrain Torres, Jesus Reyes, Nate Wilson, and Fahad Al-Ajmi for their support and friendship throughout this process.

To Javier Martinez

ABSTRACT

Renewable energy alternatives are currently of interest to meet ever-growing energy demands due to fossil fuel depletion and climate change. Biofuels, an alternative source, can be made from a range of organic matter. One option is algae, which can be grown without impacting food production and in a variety of conditions, however, the feasibility of converting algae into biofuel is of concern. Dewatering algae is a critical step in the process to make oil extraction more efficient. This study utilizes carbon dioxide clathrate hydrates as a novel process to dewater water-saturated algae solutions. Clathrate hydrates are crystalline solids formed from water molecules that contain trapped gas molecules. Carbon dioxide is specifically trapped in Structure I hydrates that are composed of a $5^{12}6^2$ structure. A stainless-steel reactor was used to perform proof-of-concept experiments using *Chlorella* sp. Experiments were performed with an initial pressure of 450 psig in a refrigerated circulator cooled to 2°C for three or more days with occasional agitation to encourage carbon dioxide hydrate formation. After performing several experiments, it was found that between 0.2 to 14.7 wt% of free water was converted into clathrate hydrates. Overall, the results show potential for the use of clathrate hydrates to dewater a water-saturated algae solution.

TABLE OF CONTENTS

LIST OF TABLES

LIST OF FIGURES

Chapter 1: INTRODUCTION

Enerdata (2019) estimates in 1990 the world used 8,561 million tons of oil equivalent (Mtoe) of energy, while in 2018 it is estimated 13,978 Mtoe of energy were used. In 2018, approximately 32% of energy consumption was from oil products. The U.S. Energy Information Administration (2017) projects that a 28% increase in world energy use will occur from 2015 to 2040. Energy sources such as coal, natural gas, and oil products like gasoline and diesel produce carbon dioxide because of their combustion, one of several greenhouse gases. The National Oceanic and Atmospheric Administration (2020) reported that the mean atmospheric global carbon dioxide concentration for January 2020 was 412.30 ppm, up 2.63 ppm from 2019. As seen in Figure 1.1, the monthly average concentrations of carbon dioxide are cyclic and are represented with the red line. These values are corrected with the average seasonal cycle with a moving average of seven adjacent season cycles shown with the black line. Figure 1.1 overall shows a trend of carbon dioxide concentrations gradually increasing with time. Other than carbon dioxide, these energy sources can emit other gas such as sulfur dioxide, nitrogen oxides, and particulates which can contribute to air pollution.

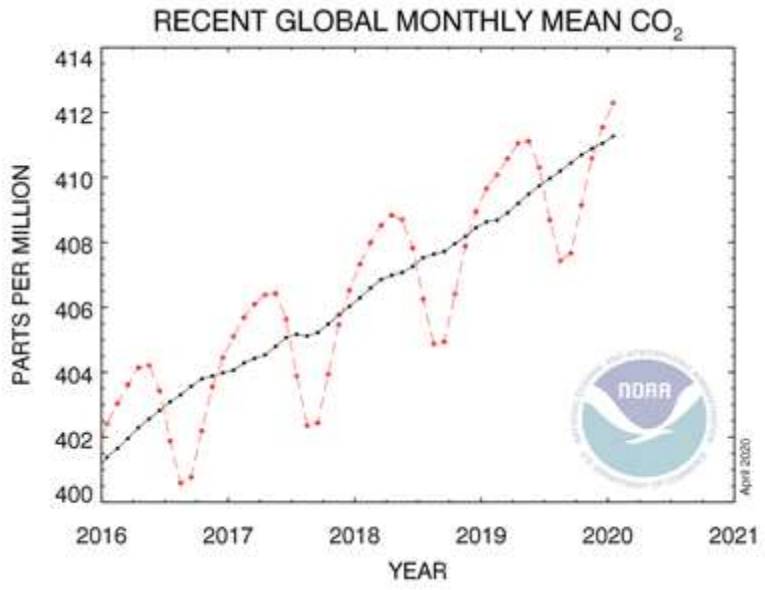

Figure 1.1 – Average Monthly Means of Carbon Dioxide (red) and Average Seasonal Cycle Monthly Caron Dioxide Concentrations (black) reported by the National Oceanic and Atmospheric Administration (2020)

Coal, natural gas, and oil products are nonrenewable resources and will eventually be depleted. When this depletion will occur can be difficult to estimate due to the annual production of these resources changing. The amount of known and reported reserves of oil resources can also change with time, impacting this estimation. Our World in Data (2017) estimates that oil reserves will be depleted in 50.7 years, natural gas reserves will be depleted in 52.8 years, and coal will be depleted in 114 years. These estimates are based on known reserves and annual production levels in 2015 which has likely changed in 2020 with the discovery of new reserves and changes in annual production. This estimate highlights that these resources will eventually run out, and though it may not be a threat to some current generations, it may be a threat to future generations.

As nonrenewable sources of energy are depleted, renewable energy alternatives are sought to reduce and potentially replace them. One potential renewable energy source is biofuels. Biofuels, such as bioethanol and biodiesel, have some current applications where they are

commonly mixed with petroleum fuels to aid in reducing emissions. Biofuels can be created from several organic materials, one of which is algae. The use of algae provides an advantage for biofuels in that it can grow in a variety of conditions such as raceway ponds, natural ponds, and wastewater. As a result, Algae does not compete with food production due, and industrial farms can utilize tubular photobioreactors to grow significantly more algae in a smaller space. Once an algal subculture has been established as harvestable, algae can be produced at rates faster than other biofuel sources such as corn. The feasibility of growing algae may be high, but the ability to use algae is low and often associated with high costs. Before using algae for biofuels, algae must be dewatered to remove excess water. This dewatering step can be costly and is often completed with the use of filtration and centrifuges.

This study proposes a novel method of dewatering algae with clathrate hydrates. This study hypothesizes that carbon dioxide hydrates can dewater a water-saturated algae solution. As clathrate hydrates are formed, gas molecules become entrapped in water cages. If a gas such as carbon dioxide is used to pressurize a system with a water-saturated algae solution and then cooled to lower temperatures, carbon dioxide hydrates should form, utilizing water molecules from the water-saturated algae solution. Eight small volume experiments were performed by pressurizing and chilling a stainless-steel reactor containing a water-saturated algae solution or algae growth medium. A windowed reactor to view hydrate formation was designed for this study, however, experiments could not be completed due to the restriction of access to the University of New Haven campus on March 9th, 2020 and then closure on March 17th, 2020 as a result of the Coronavirus Disease 2019 pandemic. Though this study may show the potential of clathrate hydrates to dewater water-saturated algae solutions, it may not prove to be a more efficient process.

Chapter 2: LITERATURE REVIEW

2.1 *Chlorella*

Due to this study's focus on a novel dewatering technique, an algae species that is commonly used for biofuel research was sought. *Chlorella* was selected due to its common use, primarily for food production, however, several studies have also utilized it for biofuel production. To find which species of *Chlorella* to use, a study performed by Guccione et al. (2014) which analyzed nine strains was reviewed. This study grew these strains in control conditions, nitrogen-starved media conditions, and high-temperature conditions. It then compared the protein, carbohydrate, lipid, and ash content of these strains. From this study, three strains were of interest due to their lipid content in nutrient sufficient and nitrogen starved mediums: *Chlorella* PROD1 which had a lipid content of 28.1±0.20%, *Chlorella* CH2 which had a lipid content of 23.1±0.03%, and *Chlorella* CCAP 211-11b which had a lipid content of 22.0±2.13%. All three strains saw significant increases in lipid content in nitrogen starved mediums with *Chlorella* PROD1 which had a lipid content of 47.4±0.06%, *Chlorella* CH2 which had a lipid content of 50.8±1.43% and *Chlorella* CCAP 211-11b which had a lipid content of 46.0±1.34%. Ultimately, using just a standard growth medium and potentially wastewater for algae growth was selected and *Chlorella* CCAP 211-11b was of interest to researchers.

The second algae species that was of interest was *Chlorella vulgaris*, one of the most used commercial microalgae (Guccione et al. 2014). *Chlorella vulgaris* was the microalgae used in a study by Yeh & Chang (2012) which reviewed how lipid content was impacted by different cultivation conditions and growth medium compositions. Three growth mediums were tested: nitrogen-rich and nutrient-rich Basal medium, nitrogen-rich and nutrient-poor Modified Bristol's Medium CZ-M1, and nitrogen-poor and nutrient-poor MBL Medium. Five cultivation conditions

were tested using 4 different energy sources and four different carbon sources: phototropic cultivation which used light and carbon dioxide, phototropic cultivation which used light and sodium bicarbonate, heterotrophic cultivation which used glucose as the energy and carbon source, photoheteromorphic cultivation which used light and glucose, and mixotrophic cultivation which used light and glucose as an energy source and carbon dioxide and glucose as a carbon source. Heterotrophic cultures and phototrophic cultures using sodium bicarbonate had low lipid productivity in all mediums. Of note, the best lipid productivity came from a mixotrophic culture in Modified Bristol's Medium CZ-M1. Modified Bristol's Medium CZ-M1 produced the highest lipid productivity overall in mixotrophic and photoheterotrophic cultures. This is of note as the composition for UTEX Proteose Medium planned to be used with UTEX 2714 *Chlorella vulgaris* is a Modified Bristol medium with Proteose Peptone added to a Bristol medium (UTEX Industries. (n.d.)a).

In a study by De-Bashan et al. (2002) synthetic wastewater was used to grow *Chlorella vulgaris* for their study to investigate whether growing *Chlorella vulgaris* with algal growth promoting *Azospirillum brasilense* would promote the microalgae removing ammonium and soluble phosphorus ions. This study found that the use of algal growth-promoting bacteria did increase uptake and proposed microalgae with growth-promoting bacteria as a novel method of treating wastewater.

2.2 Biofuels

2.2.1 Terminology

Biofuel terminology can be broken into three categories. The first category of terminology that defines blended biofuels and petroleum fuels. Ethanol from biomass, bioethanol, is often

blended with gasoline in the United States. The most common blend for transportation gasoline is E10, a 10% ethanol content by volume which most gasoline does not exceed. E15, gasoline with 15% ethanol by volume is uncommon and E85, gasoline with 85% ethanol by volume is rare (U.S. Energy Information Administration, 2019). Biodiesel commonly comes in a B5 blend, which is 5% biodiesel and 95% petrol diesel in Europe, however, some vehicles will opt to use B100, 100% biodiesel, engines can be run on both mixes and pure biodiesel, though they require more maintenance to use B100. In the United States, B20 is the common biodiesel blend, which is 20% biodiesel and 80% petrol diesel (U.S. Department of Energy, 2018).

The second category of the terminology used is descriptive terminology is used for marketing purposes (Knothe, 2010). This terminology is defining a biofuel based on its crop source generation. First-generation biofuels are biofuels that are produced from crops that also serve as food and are grown on land used for growing food. These biofuels are produced through fermentation or transesterification of oils, sugars, and starches obtained from the crops. Second-generation biofuels are produced from crops that do not serve as food or are waste from food crops. These biofuels are produced from agricultural organic waste, wood, and crops such as straw via fermentation of sugars and gasification. They are grown on land specific for biofuel production or agricultural land for biofuels that use agricultural organic waste. Third generation crops are produced from crops that do not serve as food and are grown for biofuel production such as microalgae. They are produced by oils extracted from these crops and are grown on land not used for agriculture. Fourth-generation biofuels are emerging biofuels (Alalwan et al., 2019).

The third category of terminology are standards defined by the United States Environmental Protection Agency (EPA) through the National Renewable Fuel Standard Program. This program sets requirements for how much biofuels should be blended into petroleum fuels

annually in the US. The first standard is conventional renewable biofuel. These biofuels are ethanol produced from corn starch and are required to have a life-cycle greenhouse-gas threshold emission reduction of at least 20%. The second standard is advanced biofuels. These biofuels are fuels that are produced using methods other than ethanol from corn starch. They are required to have a life-cycle greenhouse-gas threshold emission reduction of at least 50%. The third standard is a subcategory of advanced biofuels, biomass-based diesel. Biomass-based diesel is biodiesel produced from oils and fats no co-processed with petroleum sources. They are required to have a life-cycle greenhouse-gas threshold emission reduction of at least 50%. The fourth standard is a subcategory of advanced biofuels, cellulosic biofuels. Cellulosic biofuels are biofuels produced from cellulose, hemicellulose and/or lignin. They are required to have a life-cycle greenhouse-gas threshold emission reduction of at least 60%.

2.2.2 Non-Algal biofuel Crops

Biodiesel can come from several crops including corn, soybeans, algae, camelina, canola, rapeseed, jatropha, seashore mallow, peanuts, and tallow trees. Corn is America's top crop for producing fuel, however, it has significantly high costs that make its feasibility low (AGAMERICA LENDING, 2017). Soybeans are a highly researched oil and lipid source for biodiesels and biofuels with companies genetically modifying the crop to increase yields. Increasing energy demands require more studies on soybeans to increase yields and more agricultural land. Peanuts are a new oil crop under investigation for biodiesel as several states in the United States are the top producers of the crop, however, it requires fungicides to grow which increases costs. Corn, soybeans, and peanuts are examples of first-generation biofuel crops. Camelina, canola, rapeseed, and other "oilseeds" offer large oil yields, however, they require many acres to grow which competes with food crops such as wheat. Jatropha is a bush that can grow in

poor conditions that have a high oil concentration, however, it primarily grows in tropical or arid areas and poorly in other regions. The Chinese tallow tree has been looked at as an oil source due to its potential yield, but it is a rapidly growing invasive species and requires maintenance to prevent this. Seashore Mallow is an oil crop that can be grown with water of a higher saline content, unlike most other biodiesel feedstocks, however, oil yields are low (National Biodiesel Board, 2008). Oilseeds, jatropha, Chinese tallow trees, and seashore mallow are examples of second-generation biofuel crops.

2.2.3 Algal Biofuels

Algal biofuels are a third-generation biofuel. Algal biofuels used in blending typically are advanced biofuels or biomass-based biodiesel. Algae is used due to its higher theoretical oil yields when compared to other crops. Theoretical oil yields from microalgae range depending on the source. One source reports microalgae can be used to theoretically produce 2,000-5,000 gallons of biofuel per acre per year (gals biofuel/ac/yr) (ALL ABOUT algae.com 2012). DuByne (2012) reports microalgae can be used to theoretically produce 5,000-15,000 gals biofuel/ac/yr. Farm-Energy (2019) reports microalgae can theoretically produce 6,283-14,631 gals biofuel/ac/yr. However, no algae industry has been able to produce these theoretical yields. Companies have proposed expected theoretical yields, but due to costs, are unable to achieve these as less algae biomass is produced than expected. Further, some oil is lost during the extraction process through mechanical presses and hexane extraction (Wesoff, 2017).

Algae is grown in water and can be grown in compact water systems like photobioreactors. This can result in the growth of large amounts of algae in a smaller area. Raceway ponds is an alternative method for algae growth; however, this can take up land for biofuel industries or other crops. Raceway ponds are large exposed surface ovular ponds in which algae is circulated using

paddlewheels. This circulation and the bubbling of carbon dioxide prevents settling of microalgae so it can receive sunlight to grow. Tubular photobioreactors can allow algae to be grown in or close to buildings utilized by algal biofuel production industries. These systems are a vertical or horizontal tubing system that has a series of tubes connected by 180° pipe elbows. A column full of algae acts as a source for systems which enter the tubes using centrifugal pumps. Algae which enters the system travels through the tube returns to the column to receive air, carbon dioxide, and fresh medium from feed pumps. These systems, like raceway ponds, can prevent algae from settling to allow an equal distribution of light. Algae has shown some potential in growing in wastewater and can potentially be used in wastewater cleaning as suggested by De-Bashan, Moreno, Hernandez, & Bashan (2002).

Algae from raceway ponds is harvested daily once an algal culture has been established. A section of the raceway pond is quartered off and the water-saturated algal solution is pumped out. Tubular photobioreactors can collect algae in the column for use or attach piping to the tube system outlet to collect algae from the tubular portion of the system. The algae solution extracted from these systems has a high water content, which needs to be removed for more efficient oil extraction. Primary dewatering processes are used to remove bulk water and create an algal sludge and then remaining water is removed with secondary dewatering processes. Dewatering is expanded upon in Chapter 2.3.

Once algae biomass has been harvested and dewatered, oil is extracted, typically through mechanical processes. Oil presses can be used for the simplest form of oil extraction with yields of up to 75% oil. This method can be improved using hexane solvents. Algae leftover from the press is mixed with hexane which is then filtered improving yields up to 95% oil. Mechanical extraction processes are mostly used due to their simplicity and lower costs. Less common oil

extraction includes the use of supercritical carbon dioxide. Algae biomass is mixed with supercritical carbon dioxide which acts as a solvent, dissolving the biomass. Oil can be selectively extracted by controlling the pressure and temperature of the system in a fraction collector (Waters, (n.d.)). The cooling of the carbon dioxide is used to separate the oil from the carbohydrate, protein, and water contents of the algal cell. This process can extract up to 100% of oil, however at higher costs than the use of oil presses. Oil extracted from biomass is refined for use with transesterification processes where potassium hydroxide or sodium hydroxide catalysts are used to react extracted oil with an alcohol species such as methanol to produce biofuel and glycerol which is filtered out (Newman, 2020).

Several studies have reviewed the production of algal biofuels. Wu et al. (2012) concluded that microalgae biodiesel has potential in aiding with wastewater treatment and carbon dioxide fixation. This can be done by creating mixotrophic cultivation systems that utilize wastewater and the sequestration of carbon dioxide flue gas. However, improvements and developments need to be made with biorefineries and technology to enable economically feasible microalgae production. Slade & Bauen (2013) summarized that advances and the optimization of technology and production systems are needed for microalgae production. Microalgae has higher theoretical oil yields than other crops, but its biomass is ultimately more expensive to cultivate. Further environmental impacts need to be considered and mitigated in regards to water use, carbon emissions, and energy use of photobioreactor life cycles. Abishek, Patel, & Rajan (2014) summarized that biodiesel from microalgae is technologically feasible and can potentially phase out petroleum fuels. However, this study finds the economics of biodiesel from microalgae are infeasible. High lipid microalgae are needed to produced biodiesel at low costs which require genetic engineering and the use of ideal growing conditions. Thus, improvements in

photobioreactors and algae biorefineries are required for production to become feasible. Tan et al. (2018) concluded that currently used cultivation systems have a high demand for water, nutrients, and energy to grow algae, high initial costs, and chances of contamination which result in overall low economic feasibility. Hybrid semi-continuous cultivation systems that combine tubular photobioreactors and raceway ponds can potentially lower these costs while still producing high yields. Ultimately, these studies show improvement in the cultivation of algae to the production of biofuel from it. This study will focus on the dewatering stage of biofuel production.

2.3 Algae Dewatering

Once algae has been cultivated, it needs to be dewatered as a drier algae biomass makes oil extraction more efficient for physical processes. Algae is sometimes dewatered in multi-step systems for efficient dewatering. Heat is rarely used as costs from the energy required to dry algae are higher than the costs associated with dewatering (Soomro, et al., 2016). Dewatering processes can be categorized into two types: primary and secondary dewatering. Primary dewatering focuses on concentrating an algal culture from a water-saturated solution to a slurry, whereas secondary dewatering focuses on further concentrating the slurry into biomass and drying. Multiple secondary dewatering processes may be used together to improve efficiency (Sharma et al., 2013). For this study, the dewatering of algae with carbon dioxide clathrate hydrates was performed as a primary dewatering process.

The most popular dewatering technique in the algal biofuel industry is the use of centrifuges. Centrifuges are considered the most efficient recovery technique as they can process large cultures and do not require high solid content. Centrifuges, however, have a large initial capital cost and large energy costs associated with them. Occasionally, algal cells can be burst by centrifuges resulting in minor losses of oil (Soomro et al., 2016). Industries can run centrifuges as

a secondary or primary dewatering process. Other mechanical dewatering processes include flocculation, filtration, and flotation. Flocculation is a primary dewatering process that uses flocculants to dewater algae by transporting them out of the water-saturated solution to the surface of the solution. For an algal culture, this process requires large amounts of the flocculant which can drive up costs. Filtration includes a variety of secondary dewatering processes including the use of screen filters and microstrainers. These processes have good efficiency, however, the biomass product that is filtered can be impure with organic substances. These processes additionally have high capital costs and can have technical issues such as disruptive pressure changes and clogging. Flotation is a primary dewatering process that uses microair bubbles to trap microalgae. This causes the microalgae to rise to the surface but requires the use of collectors and surfactants, increasing costs and possible contamination (Sharma et al, 2013). Electrocoagulation and magnetic separation are non-mechanical dewatering processes uncommonly used. Magnetic separation uses magnetic field gradients and materials of different magnetic moments to separate algae from the water with magnetic separation. This process has good efficiency and simple operation with few technical issues. However, nanomagnetic particles needed for this process have high costs and low adsorptive capacity. Electrocoagulation is a highly selective dewatering process that has good efficiency and is described as environmentally friendly. However, due to the need for electricity and replacement of cathode and anode materials, it is additionally associated with high costs (Soomro et al., 2016).

2.4 Clathrate Hydrates

This thesis proposes the use of clathrate hydrates to dewater algae. Clathrate hydrates are naturally occurring crystalline solids that contained trapped gas molecules. The formation of clathrate hydrates occur at low temperatures under high pressure. All clathrate hydrates are

clathrate compounds that have water as their host molecule. Guest molecules for these clathrate compounds are hydrophobic moiety containing polar molecules or non-polar molecules and can be in the liquid or gas phase. Gases such as methane, carbon dioxide, and hydrogen sulfide will form clathrate hydrates. Water will form hydrogen-bonded structures around a guest molecule to form a structure called a cage. These cages can have several different geometries dependent on the trapped molecule as seen in Figure 2.1. If the guest molecule is removed from the cage, the cage will collapse (Sloan & Koh, 2008). Carbon dioxide and methane clathrates are Structure I hydrates composed of $5^{12}6^2$ cavities, while propane clathrates are Structure II hydrates composed of $5^{12}6^4$ cavities (Heriot-Watt Institute of Petroleum Engineering, 2018). Gas hydrates have been used in research to separate carbon dioxide and other gases from flue gas (Kang & Lee, 2000), to store and transport natural gas (Mimachi, et al., 2014), and in desalination processes (Fakharian, Ganji, & Naderifar, 2017). Research is being conducted in joint efforts by the United States and Japanese Governments on using naturally occurring methane hydrate deposits in the Alaska North Slope as an energy source. The research is currently attempting to investigate methods at refining and producing energy from these deposits and extend these findings to marine deposits (Department of the Interior, U.S. Geological Survey, 2017).

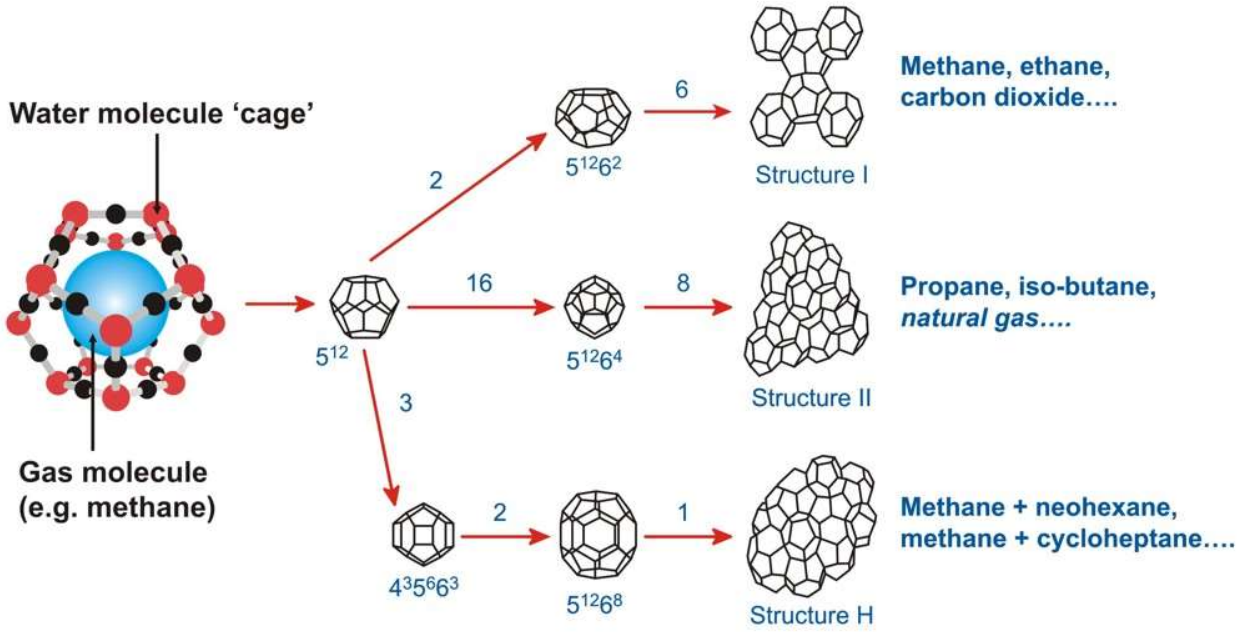

Figure 2.1 – Clathrate Hydrate Cages (Heriot Watt Institute of Petroleum Engineering, 2018).

2.5 Dewatering with Clathrate Hydrates

Clathrate hydrates have been used in a few dewatering processes. Gaarder & Englezos, (1995) attempted to form propane, carbon dioxide, and mixed gas hydrates in paper mill effluents. The mixed gass hydrates used a 30-70 mol% mixture of propane-carbon dioxide gas. This was attempted in the development of a dewatering process for paper mill effluents to recycle water. The study found that clathrate hydrates would form in the effluents in the presence of impurities, which would not impact hydrate formation. Wu et al. (2018) attempted to use the formation of propane hydrates to dewater sewage sludge. This study found that propane hydrate formation would occur in the sewage sludge and would not be impaired by contaminants. The cages of clathrate hydrates allowed the molecules to exclude sludge particles, only trapping propane. This study conducted 14 batch runs which dewatered the sewage sludge from 98.81 wt% water to 44.3 wt% water due to propane hydrate formation. These two studies show that clathrate hydrate

formation does have applicability to dewatering processes. No literature or studies were found which utilized clathrate hydrate formation for the dewatering of water-saturated algal-solutions.

Chapter 3: METHODS

3.1 Algae

3.1.1 Algae Growth Setup

Chlorella algae was selected to be grown for use in experiments in this study. To sustain the growth of the algae, a growing area was set up in a chemical hood in laboratory B310C of the University of New Haven's Buckman Hall in March 2019. This setup was later moved in October 2019 to a chemical hood in laboratory B313 of Buckman Hall. Throughout May 2019 to September 2019, the algae cultures and subcultures were kept with Dr. Amy Carlile at the University of New Haven's Charger Plaza while Buckman Hall underwent construction. For a proper setup, the algae required light to grow, containers for seeding, and a growth medium. Algae would be seeded into containers filled with the growth medium and then placed under a light to grow a subculture from the original seeding algae. An iPower 24W 2 Feet T5 Fluorescent Grow Light Stand with an adjustable hanging light was used as the light source for this setup. The light source height was adjusted until a lux meter read 3000 lux ± 100 lux, which is ideal for *Chlorella* algae growth. The selected growth medium was UTEX Proteose Medium for UTEX 2714 *Chlorella vulgaris* and Alga-Gro® Freshwater Medium for CAROLINA™ 15-3068 Concentrated *Chlorella*. Algae was seeded into a 250 mL Corning Pyrex round media storage bottle or a 4 L Corning Pyrex round media storage bottle.

In the B310C laboratory chemical hood setup, during the first month of growth in March, some media storage bottles were aerated, while some were not. For non-aerated systems, a piece of plastic airline tubing was used to connect a filter exposed to the air in the hood to a metal piece of tubing that fed into the algae medium. This metal piece of tubing was held in place via a rubber

stopper. This allowed for the algae to directly get air from the hood system. For those being aerated, as seen in Figure 3.1, air from the chemical hood was used after it passed through a filter and then through a flow meter. Airflow ranging from 50 to 70 sccm would flow into the medium through plastic tubing that connected the flow meter to metal tubing leading into the algae medium. Exhaust tubing allowed air to flow out of the media storage bottle and was connected to a piece of plastic tubing that fed into a glass beaker full of water to check if any air was leaving the system. Both pieces of metal tubing were held in place by a rubber stopper. This method was later changed to support three 250 mL media storage bottles. This was done by installing a cross connection after the flow meter and connecting tubing to the three free connections. These three pieces of tubing each connected to a respective 250 mL media storage bottle. This system was later abandoned in April 2019. Instead, small pieces of filter paper were used to cover the ends of the metal tubing held in place by a rubber stopper. This method was similar to the non-aerated method in March 2019 and was modified after discussing our methodology with Dr. Amy Carlile of the University of New Haven's Biology and Environmental Science Department. This methodology was changed in February 2020, when metal tubing was no longer used with the rubber stoppers as seen in Figure 3.2. Instead, a large piece of filter paper was placed between the cap and rubber stopper. This piece of filter paper would cover and act as a filter for the holes of the rubber stopper that once held the metal tubing that allowed air into the system. Aerating the system directly through a filter was found to provide no benefit compared to no aeration and a piece of filter paper to protect algae from dust. During the algae growth period with Dr. Amy Carlile, the algae was not aerated and showed similar growth rates to when they were aerated. As a result, aeration was abandoned, simplifying the growth system.

Figure 3.1 – March 2019 Algae Growing Setup

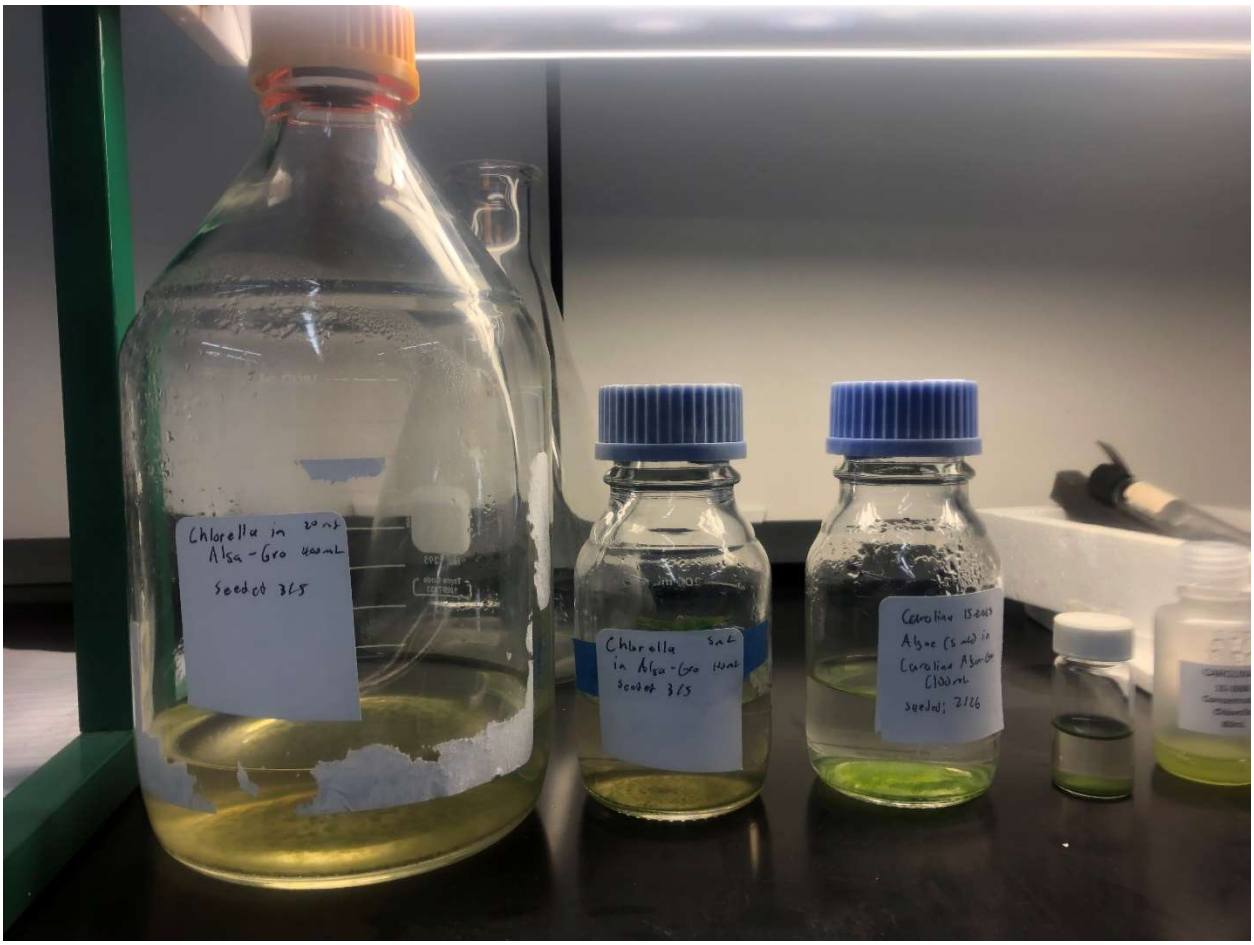

Figure 3.2 – March 2020 Algae Growing Setup

3.1.2 Algae Growth Materials Sterilization

Media storage bottles for this study required sterilization to prevent contamination during the seeding process. For this study, the selected method of sterilization was the use of an All-American 25X-120V Electric Sterilizer as an autoclave. Due to damage to the autoclave, the excess pressure relief valve was replaced before operating. The first step of the sterilization process was the cleaning of materials that were to be autoclaved. Media storage bottles were cleaned by using a bleach solution containing 5.25% sodium hypochlorite and then rinsing until no odor persisted. Media storage bottles then had a loose piece of aluminum foil placed to cover their opening. Tubing would be rinsed with a small amount of bleach and then water, assembled, and placed into

sterilization pouches. Rubber stoppers and caps were rinsed with bleach and then water. These items were then placed into beakers to be autoclaved. The first autoclaving of these items found they would become discolored. Instead these items were soaked in a bleach-water bath while other materials were autoclaved in future sterilizations. Rubber stoppers used to hold tubing were still assembled with their respective tubing and were placed into sterilization pouches. Rubber stoppers autoclaved in sterilization pouches were not discolored. Once methodology was switched to using filter paper the method of preparing the metal tubes for autoclaving changed. Metal tubing were removed from their rubber stoppers before autoclaving and rinsed with bleach and then water. Aluminum foil was then lightly wrapped around the tube and placed into a beaker.

Figure 3.3 is a model of the autoclave that can be referenced in the following operating description. Preparation of the autoclave and sterilization were performed in a chemical hood. To begin sterilization, the aluminum inner container was removed from the autoclave. Approximately 1 gallon of water was used to fill the autoclave to a height below the stainless-steel support stand. Materials were placed into the inner container which had a capacity of 14.5 qt. Several 250 mL media storage bottles could be sterilized with other materials, while the 4 L media storage bottle could only be autoclaved with sterilization pouches due to its large size. Once the inner container was loaded, it was placed back into the autoclave on top of the stainless-steel support stand. The inner container was placed to have the slot for the flexible air exhaust tube aligned with the lid. Vacuum grease was applied to the rim of the lid autoclave inner rim. The flexible air exhaust air tube was inserted into its slot and the autoclave lid was then placed on the top of the system, twisting to put the first layer of locks in place. To ensure the lid was level, it was pressed into place in a circular motion. Once this was done, the six secondary locks were used to secure the lid being tightened in a diagonal pattern to ensure all sides are level and tightly sealed.

Figure 3.3 – All-American 25X-120V Electric Sterilizer (AllAmericanCooker.Com (n.d.))

With the lid sealed, the control valve is opened by switching it vertically and power is supplied to the system. Heat setting 4 is used to heat the system and once water droplets begin to precipitate on the control valve for 5 minutes it is closed by switching it horizontally. This allowed the system to become pressurized. A light indicated if the system was heating, and if the light turns off before the system reached 17 psi, it was raised to heat setting 5. Once 17 psi is reached, the system entered the sterilization stage and a 30-minute timer was started. For safety purposes, the pressure should be controlled with the heat setting to exceed 20 psi. Once 30

minutes have passed, heat to the system was ended and the power was turned off. Heat-resisting gloves were used to open the control valve by switching it vertically. Heat-resistant gloves were used due to the steam released by the depressurization of the system. Once the steam had been released, the system was be opened and allowed to cool. Once opened, the aluminum inner container was typically removed. Any materials using aluminum foil as a cover were tightened to form a seal. Materials in sterilization pouches were kept sealed until used. The sterilization unit used in this study was prone to developing white mold, so all water was dumped and the system was cooled and cleaned.

3.1.3 UTEX 2714 *Chlorella vulgaris*

UTEX 2714 *Chlorella vulgaris* was selected to be the *Chlorella* species used in these experiments. This specie of *Chlorella vulgaris* originated in Santa fe de Bogota, Colombia from a wastewater-treatment stabilization pond. It was collected by Luz E. Gonzalez in July 1994 and then isolated in August 1994 (UTEX Industries, (n.d.)b). This strain was purchased from UTEX Industries and arrived on an agar slant culture in a test tube. Upon receiving the culture, the cap of the test tube was loosened to allow air and placed under the grow lamp. The test tube was rested upon the foam shipping container it came in to allow the full surface area of the culture to receive light.

3.1.4 UTEX 2714 *Chlorella vulgaris* Seeding

For this study, UTEX 2714 *Chlorella vulgaris* was seeded in 250 mL media storage bottles. Prior to seeding the algae, the media storage bottle, the cap to the lid, the rubber stopper with metal tubing attached, and UTEX Proteose Medium were obtained and kept nearby. Sterilized materials were kept in sterilization bags or sealed to limit the exposure to the non-sterile work environment.

Due to UTEX 2714 *Chlorella vulgaris* being cultured on an agar solution, an inoculation loop was required to obtain algae. A Bunsen burner was used to heat the inoculation loop until the metal glowed orange for 10 seconds. It was then be placed in an aluminum foil cover. The UTEX Proteose Medium was opened, and the aluminum foil removed from the 250 mL media storage bottle. Approximately 150 mL of UTEX Proteose Medium was added to the bottle and the medium was then sealed. The inoculation loop was used to take one scoop of agar with algae from the culture and add it to the medium. The culture is resealed and the rubber stopper with metal tubing was placed into the mouth of the bottle. The cap was used to seal the stopper to the bottle. Depending on the growth methodology, the metal tubing was attached to plastic tubing or small pieces of filter paper were placed inside their openings. The inoculation loop was cleaned by placing it into a shallow bleach solution and then rinsed with water.

UTEX 2714 *Chlorella vulgaris* was seeded with this methodology in March 2019. Algae grew slightly for two weeks before dying. It was seeded again later in March 2019 with a modified methodology where 2 scoops of agar with algae were used. This subculture was additionally aerated but died approximately 2 weeks after seeding. In April 2019, it was seeded one last time with a modified methodology where 3 scoops of agar with algae were used. The system was briefly aerated until May. During May this algae subculture was given to Dr. Amy Carlile along with other subcultures. During its supervision by Dr. Amy Carlile, an unidentified foreign mass grew suggesting there was some form of contamination. Due to the slow-growing speed and resulting contamination of subcultures that grew, this species of *Chlorella* was never used in this study due to its unreliability.

3.1.5 CAROLINA™ 15-3068 Concentrated *Chlorella*

In April 2019, due to the slow speed of growth from UTEX 2714 *Chlorella vulgaris*, a secondary, faster-growing algae culture was sought to be used in experiments. CAROLINA™ 15-3068 Concentrated *Chlorella* was selected being an unspecified strain of *Chlorella*. This algae culture was bought from Carolina Biological Supply Company and arrived in a liquid medium with a total volume of 60 mL. Upon receiving the culture, the cap was loosened to allow the bottle to get air and placed under the grow lights. Once per day, the bottle was agitated due to settling. This algae culture would be used to create subcultures used for experimental runs in this study. The algae culture was additionally used in its own set of experimental runs.

3.1.6 CAROLINA™ 15-3068 Concentrated *Chlorella* Seeding

The seeding of CAROLINA™ 15-3068 Concentrated *Chlorella* used a modified methodology of the seeding of UTEX 2714 *Chlorella vulgaris*. In this modified methodology, 125 mL ± 50 mL of Alga-Gro® Freshwater Medium is used as the algal growth medium. An inoculation loop is not needed for seeding as the culture is a liquid. A 7 mL sample of concentrated *Chlorella* culture is added to the medium via a syringe as recommended by Carolina Biological Suppy Company. In March 2020, this methodology was modified to use 5 mL of CAROLINA™ 15-3068 Concentrated *Chlorella* and 100 mL of Alga-Gro® Freshwater Medium for seeding.

Methodology was modified to seed the 4 L media storage bottle. A ratio of 60 mL of concentrated *Chlorella* culture to 1000 mL of algal growth medium was used to first seed this media storage bottle in April 2019. In March 2020, the ratio of 5 mL of concentracted *Chlorella* culture to 100 mL of algal growth medium was used for 400 mL. Due to the lengths of the metal

tubing being significantly shorter than the height of the 4 L media storage bottle, only a rubber stopper with a large piece of filter paper was used.

A study performed by Danielle Belskis, an undergraduate student conducting research with Dr. Kristine Horvat, on algae flocculation and algae growth in synthetic wastewater was performed simultaneously to this study. Algae used in Danielle Belski's study was the same algae used in this study. As part of their study, synthetic wastewater was prepared and used in place of Alga-Gro® Freshwater Medium in April 2019. Due to CAROLINA™ 15-3068 Concentrated *Chlorella* not being able to survive in this wastewater, algae grown in wastewater was not used in this study. To test Danielle's flocculation methods, a large subculture of algae was prepared in the 4 L media storage bottle in April 2019. This preparation followed a similar methodology described, however, it used 1 L of Alga-Gro® Freshwater Medium and 60 mL of CAROLINA™ 15-3068 Concentrated *Chlorella*. This subculture would be one source of algae used in this study.

In March 2019, two 125 mL CAROLINA™ 15-3068 Concentrated *Chlorella* subcultures were prepared for a study being performed by Danielle Belskis, one of which contained synthetic wastewater. This was repeated in April 2019 with the preparation of a 1 L CAROLINA™ 15-3068 Concentrated *Chlorella* subculture in Alga-Gro® Freshwater Medium. In May 2019, two 125 mL CAROLINA™ 15-3068 Concentrated *Chlorella* subcultures with Alga-Gro® Freshwater Medium. The 1000 mL subculture would be used for carbon dioxide hydrate experiments and one 125 mL subculture would be used for drying experiments. In February 2020, two 100 mL and one 400 mL CAROLINA™ 15-3068 Concentrated *Chlorella* subcultures using the new ratio of 5 mL algae solution to 100 mL of algae growth medium were prepared. Due to the death of the 400 mL and one 100 mL subculture, in early March 2020, one 100 mL and one 400 mL CAROLINA™ 15-3068 Concentrated *Chlorella* subcultures were created. Due to the restriction of access to the

University of New Haven campus on March 9th, 2020 and then closure on March 17th, 2020 as a result of the Coronavirus Disease 2019 pandemic, these subcultures were not used in this study.

3.1.7 Determination of Weight and Density

Using a 125 mL subculture of CAROLINA™ 15-3068 Concentrated *Chlorella*, the weight of the dry algae mass of the subculture could be found. A tray dryer in B310C in Buckman Hall was utilized in September 2019. The algae subculture solution was distributed onto three drying trays and massed. They were then placed on the drying rack inside the tray dryer. The airflow control was set to velocity setting 7 which resulted in an average air velocity of 1.1 m/s. The temperature control was also set to heating setting 7 which resulted in an average temperature of 32.4°C before the drying rack and 35.6°C after the drying rack. The total time of drying was 5.7 hours. This resulted in all medium being evaporated. Dry algae were removed from each tray by scraping the algae with a laboratory spatula. This mass was collected in a vial and weighed; however, it represents an underestimate as it was difficult to collect all the algae dried to the tray. Figure 3.4 shows the algae spread onto drying trays before and after this drying process.

Figure 3.4 – Algae Spread onto one of the Drying Tray before Drying (left) and after Drying (Right)

The density of the algae solution is important for calculations on how much water is used in the formation of algae hydrates. An average density was found for algae by determining the mass of 200 mL of CAROLINA™ 15-3068 Concentrated *Chlorella* subcultures contained in a beaker. This method was repeated on three 200 mL samples for each experimental run, and these densities were averaged to be used in calculations. An average density was used due to the algae collection process, as the density of the 15 mL of algae solution collected from the beaker would vary slightly from the original bulk density of the 200 mL algae solution. This is due to the lack of uniformity in the size and distribution of algae in the solution due to the varied particle growth of the subculture.

3.2 Gas Hydrate Experiments

3.2.1 Small Volume Reactor

Small volume experiments were performed using a gas hydrate reactor as seen in Figure 3.5. This reactor is created from 8" of windowless stainless-steel tubing connected to two 1" fittings. The bottom 1" fitting allowed the reactor to be emptied from the bottom. The top 1" fitting is an adapter connecting a piece of ¼" stainless-steel tubing to the reactor. This ¼" tubing is connected to a Swagelok quick connect fitting to allow for easy opening. A separate top assembly portion of the system contained a pressure transducer and thermocouple. During experiments, a 15 mL sample was added to the 1" reactor through the ¼" piece of tubing. Stacie Meruelo, a previous undergraduate research student for Dr. Kristine Horvat, previously estimated the working volume of the reactor to be 79.31 mL calculated from measured lengths and known diameters of the reactor parts.

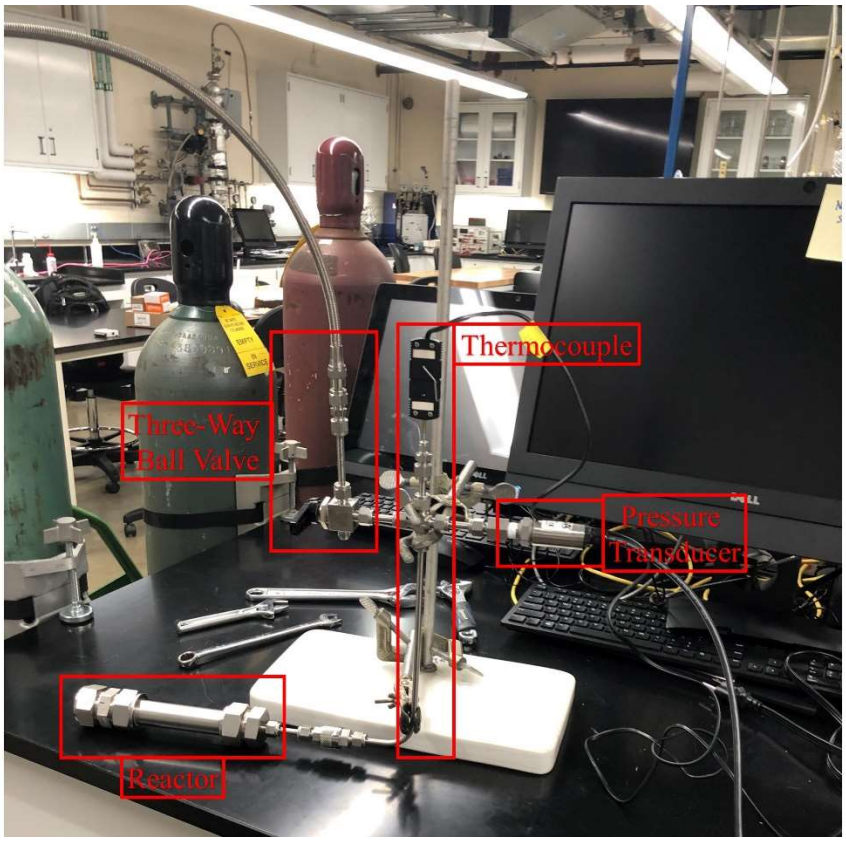

Figure 3.5 – Small Volume Reactor

The top assembly of this reactor connects to a stainless-steel tubing system that allows for the pressurization of the reactor. This tubing system contains a thermocouple to measure the temperature inside the reactor and a pressure transducer to track the pressure of the reactor. The thermocouple runs through the middle of a cross connection through the tubing system's quick connect. To connect the quick connect fittings, the thermocouple must first be inserted into the ¼" stainless-steel portion of the reactor. A pressure transducer and a three-way valve are connected to the other two sides of the cross connection. The three-way valve is used to either pressurize the system when connected to a gas cylinder or depressurize the system at the end of an experiment.

3.2.2 Gas Hydrate See-Through Reactor

A second reactor was designed and planned to be used after the small volume reactor experiments. This reactor utilizes a Jerguson 19T32 level gage as the body of the reactor sold by Jerguson Gage & Valve Company. It features see-through windows on two sides, allowing the hydrate formation process to be seen. The borosilicate windows of this reactor are 34 mm thick with a 340 mm length on both sides. The visible viewing length of the windows is 321 mm and the overall length of the system is 359 mm or 14.125". As a result, there is a slightly larger working volume (just under 200 mL) with this reactor than the small volume reactor. The T-32 series was selected as the windows are transparent and the system can withstand pressure up to 4000 psi at 100°F, well within our operating conditions for carbon dioxide hydrates and future methane hydrate experiments.

To track the pressure and temperature needed to study the formation of gas hydrates a tubing system was designed to be attached to the Jerguson 19T32 level gage to connect the gauge to a gas cylinder for pressurization. On both ends of the level gage are ¾" Swagelok stainless-steel full flow quick connect stems to easily connect the Jerguson 19T32 level gage to the tubing. The top part of the reactor will be a tubing system that reduces from ¾" stainless-steel tubing to ¼" stainless-steel tubing through a Swagelok stainless steel reducing union tee. A tee is used to allow a thermocouple to enter the reactor from the top and allow gas to enter the system. The ¼" tubing connects to a ¼" female branch tee which will have a pressure gauge attached to the branch. After the tee, the tubing continues to a Swagelok stainless-steel high-pressure 6000 psia proportional relief valve and then a Swagelok stainless-steel 1-piece 40G series ball valve for system depressurization. The bottom quick connect fitting will attach to another tubing system. This tubing system will start similarly with ¾" stainless steel tubing connecting to Swagelok ¾" to ¼"

branch reducing union tee. A tee is used to accommodate the length of the thermocouple. The ¼" stainless steel tubing connects to a Swagelok stainless steel in-line particulate filter with a pore size of 2 microns to filter gas entering the system. A Swagelok stainless steel poppet check valve is next to control the flow of gas to one direction towards the reactor. To allow gas to enter the system, at the end of this ¼" stainless-steel tubing is another Swagelok 1-piece 40G series ball valve that connects to a Swagelok stainless-steel 40G series 3-way ball valve. The 3-way ball valve is where the system will connect to a gas cylinder to allow the system to be pressurized.

In February 2020, the Jerguson 19T32 Gage arrived, along with all Swagelok parts to assemble the tubing system. However, due to a strip of waste metal attached to a borosilicate window, it was shipped back to the manufacturer, Clark Reliance, and once the University of New Haven mailroom reopens, it will be received, assembled, and leak tested.

3.2.3 Leak Testing

Gas hydrate formation is evidenced in an experiment by a pressure drop, indicating that gas has entered the hydrate phase. To ensure that pressure drop is only due to the reactor cooling, carbon dioxide solubility, and the formation of gas hydrates, leak tests were performed. Leak tests were performed with the small volume reactor after experimental runs that required the removal of the 1" reactor end cap. To perform a leak test, nitrogen gas was used instead of carbon dioxide. Nitrogen gas is a smaller molecule than carbon dioxide and allows the reactor to be tested more efficiently for an airtight seal. The small volume reactor was connected to the tubing system and then held in place by a lab stand and clamps. A blast shield was placed in front of the system and Swagelok flex tubing was used to connect the 3-way valve of the tubing system to a nitrogen gas cylinder. The pressure transducer and thermocouple were connected to the LabVIEW system which was then connected to a LabVIEW data acquisition program that tracked the pressure and

temperature of the system. The valves of the tubing system and flex tubing system are opened. The nitrogen gas cylinder is opened to allow the system to be pressurized. Though the carbon dioxide experiments were pressurized to 450 to 460 psig, the leak tests were pressurized to 660 to 670 psig. A higher pressure was selected to perform leak tests over a shorter time than experimental runs. Additionally, the higher pressure can better test for leaks with more due to more pressure against airtight seals. Once pressurized the valves to the system were closed and the nitrogen gas cylinder was closed. The flex tubing line was depressurized and then removed from the system. Leak tests were performed for 6 to 7 hours to track how pressure changes over time and if any leaks occur. Once the leak test ends, the reactor system was depressurized. The first was in October 2019 before experimental Runs 1, 2, 3, and 4. The second leak test was performed in November 2019 before Run 5. The third leak test was performed in February 2020, before Runs 6, 7, and 8. All leak tests showed that there were no leaks, as any pressure fluctuations were correlated with changes in temperature.

3.2.4 Small volume Experiments

To test if the formation of gas hydrates could dewater an algal solution, small volume experiments were performed. A total of water-saturated algal solution runs and two algal growth medium control runs were performed. Small volume Runs 1, 3, and 5 used algae from the 1 L CAROLINA™ 15-3068 Concentrated *Chlorella* subculture. Control Runs 2 and 4 used only pure Alga-Gro® Freshwater Medium as a control. Small volume Runs 6, 7, and 8 used algae from the same CAROLINA™ 15-3068 Concentrated *Chlorella* culture. Water was not used, as previous carbon dioxide hydrate formation using water was performed in previous research by Stacie Meruelo when performing research on the impact of sand on hydrate formation with Dr. Kristine Horvat.

The general methodology for runs was to first load the algae or algae growth medium solution into the reactor. For runs using algae from the 1 L CAROLINA™ 15-3068 Concentrated *Chlorella* subculture used a different method than runs using Alga-Gro® Freshwater Medium and algae from the same CAROLINA™ 15-3068 Concentrated *Chlorella* culture. To collect 15 mL of algae solution from the 1 L CAROLINA™ 15-3068 Concentrated *Chlorella* subculture, the subculture was agitated and then 200 mL of the subculture was poured into a beaker after it was weighed empty. The mass with the subculture was then weighed and several plastic disposal pipettes were obtained. Using the pipette, the solution is agitated, and 0.5 mL of algal solution was collected. The pipette was then placed at the opening of the quick connect fitting and was used to inject the solution into the reactor. Increments of 0.5 mL are added one at a time to prevent spills. If the solution does not enter the reactor, a thin piece of airline tubing was used to aid the solution in entering the reactor. This was repeated until 15 mL had entered the reactor. This system must be used due to the variety of sizes of algae in the solution. For runs using Alga-Gro® Freshwater Medium and algae from the CAROLINA™ 15-3068 Concentrated *Chlorella* culture, a syringe with a thin piece of airline tubing to extend its needle was used to collect 15 mL of the solution. The airline tubing was then inserted into the ¼" stainless-steel tubing and the solution was injected into the system.

Once the solution was loaded into the reactor, it was then attached to the tubing system via quick connect fittings. A lab stand and clamps were used to hold the reactor horizontally, parallel with the table. The pressure transducer and thermocouples were then connected to the LabVIEW system to track the pressure and temperature of the system and refrigerated circulator solution. The reactor was then connected to a carbon dioxide gas cylinder using Swagelock flex tubing and a blast shield was placed in front of the system. All valves were then opened to allow the flow of

gas into the reactor. The carbon dioxide gas cylinder was then opened to pressurize the system to 450 to 460 psig. The valves were closed and the system is agitated to allow a pressure drop from this solubility of carbon dioxide in water. Valves were reopened after this agitation and the system was pressurized to 450 to 460 psig. The valves were then closed and the carbon dioxide gas cylinder is closed. The flex tubing line is then depressurized and removed from the system. The reactor system was removed from the lab stand and was then placed into the refrigerated circulator, with the reactor laying horizontally on the floor of the refrigerated circulator. The tubing assembly was kept out of the refrigerated circulator. Before it was used, the refrigerated circulator was filled with approximately 7 gal of 50% ethylene glycol and water by volume. The lab stand and clamps were used to secure the reactor system and the refrigerated circulator cover was placed to protect the solution from dust. The thermocouple that collects the temperature of the chill was inserted through the cover and the refrigerated circulator was then powered on with the temperature set to 2°C. Figure 3.6 shows the reactor submerged in the refrigerated circulator.

Figure 3.6 – Small Volume Reactor Submerged in Refrigerated Circulator

Temperature and pressure data were collected for approximately three days using the LabVIEW program. This was not true for Run 5 which ran for approximately 16 days. Due to the desktop computers used, the program was occasionally restarted to avoid having large data files. As the LabVIEW program runs a lag began to develop in the time step used to collect data and after several hours it had begun to exceed three seconds. To attempt to minimize this, the program was restarted at least two times a day. After the first day of data collection, the reactor was removed from the refrigerated circulator to agitate the reactor. The system was agitated several more times after the initial agitation. This agitation was performed to promote the formation of carbon dioxide hydrates. Agitation was performed by an operator manually shaking the reactor.

After the three days of temperature and pressure data collection during hydrate formation, the system undergoes the dissociation stage. The pressure in the system was released to drop the pressure in regular steps. The pressure and temperature of the system were monitored to see if the pressure changes as the temperature returned to the temperature of the refrigerated circulator. The dissociation process started with steps of 25 psig where if the experimental pressure ends above 350 psig, the pressure is first dropped to 350 psig. Once the reactor temperature returned to the temperature of the refrigerated circulator, the system was then dropped to 325 psig. A series of 25 psig pressure drops were repeated until the system reached 225 psig. Once at 225 psig, the pressure was dropped to 215 psig. At 215 psig range, the increment of pressure drops was changed to 5 psig as the equilibrium pressure for carbon dioxide hydrates at 2°C is between 214 and 216 psig. For this study, this system typically attempted to approach 212 to 214 psig instead of known carbon dioxide equilibrium pressures. The 5 psig incremental pressure drop was used until the system reached 185 psig. These incremental steps usually take longer for the temperature to return to the surrounding temperature and pressures attempt to reach between 212 and 214 psig to remain at carbon dioxide hydrate equilibrium. The next incremental step was reducing the pressure from 185 to 175 psig. After this step, the pressure was slowly reduced to 0 psig. Temperature and pressure data from the dissociation process were collected in a separate excel sheet and used to plot the pressure-temperature equilibrium curve of carbon dioxide hydrate formation.

After dissociation, the reactor system was removed from the refrigerated circulator which was turned off. The outside of the reactor was cleaned and then disconnected from the tubing system that was cleaned separately. To empty the reactor, it was agitated to collect the algae solution in a vial. For some experimental runs, the reactor was emptied by removing the bottom fitting of the reactor. The reactor was rinsed thoroughly with deionized water, and air was blown

through the reactor to dry it. The tubing system was cleaned similarly with the quick connect rinsed with deionized water and then air was used to dry it. The algae solution collected from the reactor was then placed under the grow light.

Chapter 4: RESULTS

4.1 Determination of Experimental Run Characteristics

After the completion of an experiment several Microsoft Excel files containing temperature and pressure data versus time were compiled into one collective Microsoft Excel file. This was performed for each run to plot temperature and pressure data as functions of time to characterize each experimental run. For each run, several pieces of data were collected. The total run time, t_r, was the duration of the experiment. The time of when the system equilibrated at the bath temperature, t_F, was determined by finding at what time this temperature occurred for the reactor. The flatline temperature, T_F, was the temperature of the refrigerated circulator at the end of the experiment which the system equilibrates to. The time of when the first temperature peak, t_p, was determined by finding the time at which the temperature was the highest and a pressure drop followed within an hour. The induction time, t_I, was how long it takes for clathrate hydrate formation to occur once the reactor reaches the flatline temperature. Equation (1) was used to calculate the induction time.

$$t_I = t_p - t_F \textbf{ (1)}$$

4.2 Determination of Water Uptake

To determine the water uptake, the volume of the reactor, V_R, must be determined, and the volume of the solution, V_s, used in an experiment is needed. From these values, the volume of gas, V_G, was calculated by equation (2).

$$V_G = V_R - V_s \textbf{ (2)}$$

The temperature of the reactor at the initial pressure, T_i, and the flatline temperature, T_F, were determined. Three pressure values must be determined: the initial pressure, Pi, the pressure at the flatline temperature, P_F, and the pressure at the end of the experiment, P_f. Equation (3) was used to find the overall change in pressure, ΔP_E, from these values. This pressure drop was for the entire experiment, and can be broken into different stages: the pressure drop from the reactor experiencing changes in temperature, ΔP_T, the pressure drop from the solubility of carbon dioxide, ΔP_{CO2}, and the pressure drop from hydrate formation, ΔP_H. This can be represented with Equation (4).

$$\Delta P_E = P_i - P_f \textbf{ (3)}$$

$$\Delta P_E = \Delta P_T + \Delta P_{CO2} + \Delta P_H \textbf{ (4)}$$

Using Gay-Lussac's Law, Equation (5), the theoretical pressure of the reactor at the flatline temperature, P_c, was determined.

$$P_c = P_i \frac{T_F}{T_i} \textbf{ (5)}$$

This theoretical pressure was used to find the pressure drop of the reactor from changes in temperature underwent by the system using Equation (6).

$$\Delta P_{CO2} = P_i - P_c \textbf{ (6)}$$

The change in pressure from the solubility of carbon dioxide was found using isothermal carbon dioxide solubility curves created for several temperatures. Solubility was estimated from equations of best-fit lines of these solubility curves seen in Figure 4.1. Using the initial pressure and temperature, a best fit temperature curve equation was selected, and the solubility was calculated based on the pressure. This solubility was then used to find the mass and moles of

carbon dioxide that was soluble. The volume of the soluble carbon dioxide was found and using the Ideal Gas Law, the pressure of the soluble carbon dioxide was found at the initial temperature and pressure, $P_{CO2,\,i.}$ This process was repeated but used the temperature and pressure of the flatline conditions to find the pressure of the soluble carbon dioxide at these values, $P_{CO2,\,F}$. To obtain the pressure drop from carbon dioxide solubility equation (7) was used.

$$\Delta P_{CO2} = P_{CO2,F} - P_{CO2,i} \textbf{ (7)}$$

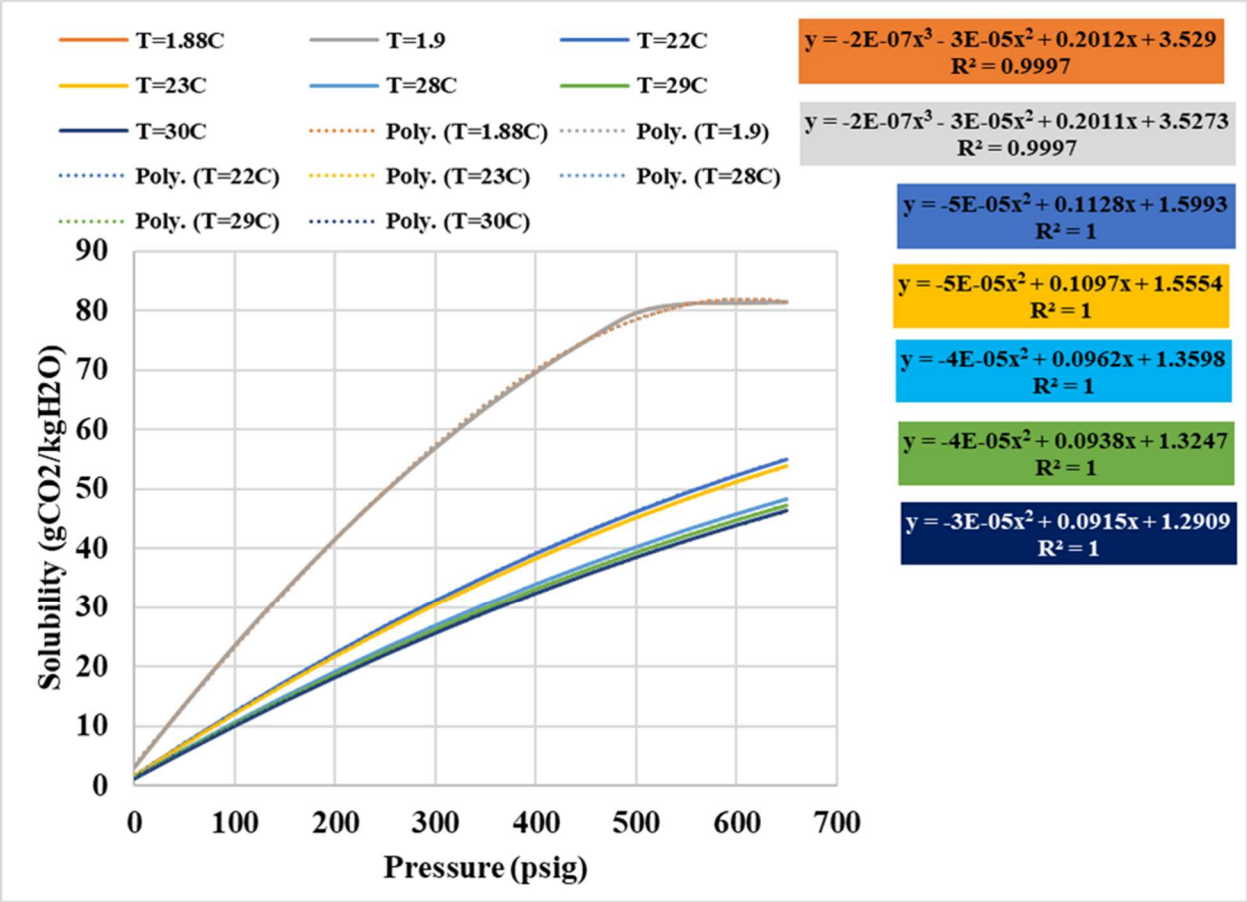

Figure 4.1 – Example Isothermal Solubility Curves and Modeling Equations

The pressure drop from hydrate formation was estimated from the overall pressure drop, the pressure drops from the temperature underwent by the reactor, and the pressure drop from carbon dioxide solubility in the solution. Equation (8) is a modification of Equation (4) to solve

for the pressure drop from hydrate formation. Due to a theoretical solubility pressure drop being used, a range was used for the hydrate formation pressure drop. The minimum pressure drop from hydrate formation was the pressure drop calculated by Equation (8). The maximum pressure drop from hydrate formation is also calculated by Equation (8); however, the pressure drop from carbon dioxide solubility was treated as zero and will be labeled Equation (9).

$$\Delta P_{H,min} = \Delta P_E - \Delta P_T - \Delta P_{CO2} \textbf{ (8)}$$

$$\Delta P_{H,max} = \Delta P_E - \Delta P_T \textbf{ (9)}$$

The Ideal Gas Law can then be used to estimate the moles of carbon dioxide gas used in hydrate formation, $n_{CO2,\,H}$. Based on the pressure drop from hydrate formation, the volume of carbon dioxide, and the flatline temperature, Equation (10) can be used to determine the number of moles. The moles of carbon dioxide used in hydrate formation can be used to determine the mass of water used by hydrate formation, $m_{H2O,\,H}$, with Equation (11). The theoretical ratio of moles of water to moles of carbon dioxide is 6:1 for carbon dioxide hydrate formation (Sloan & Koh, 2008). The molecular mass of water was represented by the term MW_{H2O}. Equation (12) can then be used to calculate the weight percent of water used in hydrate formation from the algal solution, $wt\%_E$. For the solution, the density of the algae or algae medium solution, ρ_A, was used instead of the density of water. All equations were used for both the maximum and minimum pressure drop from hydrate formation.

$$n_{CO2,H} = \frac{(\Delta P_H)V_G}{RT_F} \textbf{ (10)}$$

$$m_{H2O,H} = 6MW_{H2O}n_{CO2,H} \textbf{ (11)}$$

$$wt\%_E = \frac{m_{H2O,H}}{\rho_A V_S} \textbf{ (12)}$$

In addition to determining the experimental weight percent of the water removed by hydrate formation for each experiment, the theoretical maximum weight percent of the water removed by hydrate formation was calculated for each experiment. Other than calculating each maximum theoretical value by the maximum and minimum hydrate formation pressure drop, a calculation was done for both conditions where carbon dioxide gas is in excess and where water is in excess. To find the maximum possible weight percent conversion when carbon dioxide gas is in excess, $wt\%_{T,\ CO2}$, Equation (13) is used. To find the maximum possible weight percent conversion when water is in excess, $wt\%_{T,\ H2O}$, Equation (14) is used. These equations were used for both the maximum and minimum pressure drops from hydrate formation.

$$wt\%_{T,CO2} = \frac{(\frac{(\Delta P_H)V_G}{RT_F})MW_{CO2}}{(\frac{V_S\rho_W}{6MW_{H2O}})MW_{CO}} = \frac{n_{CO2,H}}{\frac{V_S\rho_W}{6MW_{H2O}}} \quad \textbf{(13)}$$

$$wt\%_{T,CO2} = \frac{(\frac{(\Delta P_H)V_G}{RT_F})MW_{CO2}}{(\frac{P_iV_G}{RT_i})MW_{CO2}} = \frac{n_{CO2,H}}{\frac{P_iV_G}{RT_i}} \quad \textbf{(14)}$$

4.3 Determination of Carbon Dioxide Hydrate Equilibrium in Water

The software program CSMHYD developed by Professor E. Dendy Sloan of the Colorado School of Mines was used to collect equilibrium curves for carbon dioxide hydrates. This program predicts the pressure of stable clathrate hydrates at a given temperature. These predictions were recorded and can be used to create equilibrium curves for hydrate formation by plotting pressure versus temperature. Equilibrium curves were found for pure water, water containing 0.11 wt% sodium chloride, and water containing 0.20 wt% sodium chloride. Equilibrium data were collected in 0.1°C increments from -0.5°C to 2.5°C. These salt concentrations were selected due to the unknown salt content of Carolina® Alga-Gro Freshwater Medium and algal solutions. Pure water

with no salt acted as a control curve in the scenario that algal solutions were potentially devoid of salts from the use of them for growth. Originally a concentration of 0.10 wt% sodium chloride was planned to be used, but due to the CSMHYD model, 0.11 wt% was used. This amount of salt represented the predicted salt content of an algal solution that may still have some leftover salts for algal cell growth. Lastly, it was theorized the Carolina® Alga-Gro Medium likely contained 0.20 to 0.30 wt% salt based on public growth media compositions; thus 0.20 wt% sodium chloride was selected to represent that prediction. For this study, the equilibrium curve from 1.0°C to 1.8°C was of interest.

4.4 Solution Densities

The mean density of the CAROLINA™ 15-3068 Concentrated *Chlorella* subculture was 0.9509 g/mL. The mean density of the CAROLINA™ 15-3068 Concentrated *Chlorella* culture was 0.9837 g/mL. The mean density of the Alga-Gro® Freshwater Medium was 0.9921 g/mL.

4.5 Run Summaries

In total, eight stochastic small volume reactor runs were conducted as seen in Table 4.1.

Table 4.1 – Experimental Run Summary

Run Order	Solution	Algae	Total Run Time (h)	Induction Time (h)	Agitation?	Water Uptake%	
						Min	Max
1	*Chlorella* grown in Alga-Gro	Yes	74.6	21.0	Yes	0.2%	8.0%
2	Alga-Gro	No	72.1	29.2	Yes	1.8%	9.4%
3	*Chlorella* grown in Alga-Gro	Yes	67.8	20.5	Yes	5.1%	12.9%
4	Alga-Gro	No	71.6	22.8	Yes	4.2%	12.0%
5	*Chlorella* grown in Alga-Gro	Yes	382.0	162.1	Yes	4.1%	11.5%
6	Carolina 15-2068 Concentrated *Chlorella*	Yes	71.1	20.8	Yes	7.3%	14.7%
7	Carolina 15-2068 Concentrated *Chlorella*	Yes	70.8	21.4	Yes	1.9%	8.7%
8	Carolina 15-2068 Concentrated *Chlorella*	Yes	72.4	21.5	Yes	5.7%	12.8%

4.5.1 Run 1

Run 1 used 15 mL of CAROLINA™ 15-3068 Concentrated *Chlorella* subculture. The system was pressurized to 451 psig at 23.38°C. This experiment achieved a flatline temperature of 1.81°C and a flatline pressure of 368 psig after 3.3 hours. The system was agitated and resulted in a temperature peak occurring after 24.3 hours for a total induction time of 21.0 hours. After an experimental run of 74.6 hours, the system ended at 349 psig. The calculated water removal by hydrate formation is 0.2 wt% to 8.0 wt%. In a system with excess carbon dioxide gas, the theoretical water removal by hydrate formation is estimated to be 0.2 wt% to 7.6 wt%. In a system with excess water, the theoretical water removal by hydrate formation is estimated to be 0.4 wt% to 13.5 wt%.

4.5.2 Run 2

Run 2 used 15 mL of Alga-Gro® Freshwater Medium. The system was pressurized to 453 psig at 23.82°C. This experiment achieved a flatline temperature of 1.79°C and a flatline pressure of 371 psig after 3.4 hours. The system was agitated and resulted in a temperature peak occurring after 32.6 hours for a total induction time of 29.2 hours. After an experimental run of 72.1 hours, the system ended at 338 psig. The calculated water removal by hydrate formation is1.8 wt% to 9.4 wt%. In a system with excess carbon dioxide gas, the theoretical water removal by hydrate formation is estimated to be 1.7 wt% to 9.3 wt%. In a system with excess water, the theoretical water removal by hydrate formation is estimated to be 3.1 wt% to 16.4 wt%.

4.5.3 Run 3

Run 3 used 15 mL of CAROLINA™ 15-3068 Concentrated *Chlorella* subculture. The system was pressurized to 451 psig at 23.23°C. This experiment achieved a flatline temperature of

1.82°C and a flatline pressure of 369 psig after 3.4 hours. The system was agitated and resulted in a temperature peak occurring after 23.9 hours for a total induction time of 20.5 hours. After an experimental run of 67.8 hours, the system ended at 316 psig. The calculated water removal by hydrate formation is 5.1 wt% to 12.9 wt%. In a system with excess carbon dioxide gas, the theoretical water removal by hydrate formation is estimated to be 4.9 wt% to 12.3 wt%. In a system with excess water, the theoretical water removal by hydrate formation is estimated to be 8.6 wt% to 21.7 wt%.

4.5.4 Run 4

Run 4 used 15 mL of Alga-Gro® Freshwater Medium. The system was pressurized to 452 psig at 24.13°C. This experiment achieved a flatline temperature of 1.81°C and a flatline pressure of 368 psig after 3.6 hours. The system was agitated and resulted in a temperature peak occurring after 26.1 hours for a total induction time of 22.8 hours. After an experimental run of 71.6 hours, the system ended at 319 psig. The calculated water removal by hydrate formation is 4.2 wt% to 12.0 wt%. In a system with excess carbon dioxide gas, the theoretical water removal by hydrate formation is estimated to be 4.2 wt% to 11.9 wt%. In a system with excess water, the theoretical water removal by hydrate formation is estimated to be 7.4 wt% to 21.0 wt%.

4.5.5 Run 5

Run 5 used 15 mL of CAROLINA™ 15-3068 Concentrated *Chlorella* subculture. The system was pressurized to 455 psig at 22.16°C. This experiment achieved a flatline temperature of 1.82°C and a flatline pressure of 371 psig after 3.0 hours. The system was agitated and resulted in a temperature peak occurring after 165.1 hours for a total induction time of 162.1 hours. After an experimental run of 382.0 hours, the system ended at 331 psig. The calculated water removal by

hydrate formation is 4.1 wt% to 11.5 wt%. In a system with excess carbon dioxide gas, the theoretical water removal by hydrate formation is estimated to be 3.9 wt% to 10.9 wt%. In a system with excess water, the theoretical water removal by hydrate formation is estimated to be 6.8 wt% to 19.0 wt%.

4.5.6 Run 6

Run 6 used 15 mL of CAROLINA™ 15-3068 Concentrated *Chlorella* culture. The system was pressurized to 456 psig at 22.42°C. This experiment achieved a flatline temperature of 1.80°C and a flatline pressure of 377 psig after 3.2 hours. The system was agitated and resulted in a temperature peak occurring after 24.0 hours for a total induction time of 20.8 hours. After an experimental run of 71.1 hours, the system ended at 306 psig. The calculated water removal by hydrate formation is 7.5 wt% to 11.5 wt%. In a system with excess carbon dioxide gas, the theoretical water removal by hydrate formation is estimated to be 7.4 wt% to 14.5 wt%. In a system with excess water, the theoretical water removal by hydrate formation is estimated to be 12.9 wt% to 25.3 wt%.

4.5.7 Run 7

Run 7 used 15 mL of CAROLINA™ 15-3068 Concentrated *Chlorella* culture. The system was pressurized to 456.3 psig at 21.04°C. This experiment achieved a flatline temperature of 1.82°C and a flatline pressure of 378 psig after 3.15 hours. The system was agitated and resulted in a temperature peak occurring after 24.5 hours for a total induction time of 21.4 hours. After an experimental run of 70.8 hours, the system ended at 348 psig. The calculated water removal by hydrate formation is 1.9 wt% to 8.7 wt%. In a system with excess carbon dioxide gas, the theoretical water removal by hydrate formation is estimated to be 1.9 wt% to 8.5 wt%. In a system

with excess water, the theoretical water removal by hydrate formation is estimated to be 3.3 wt% to 14.9 wt%.

4.5.8 Run 8

Run 8 used 15 mL of CAROLINA™ 15-3068 Concentrated *Chlorella* culture. The system was pressurized to 455 psig at 22.24°C. This experiment achieved a flatline temperature of 1.81°C and a flatline pressure of 370 psig after 2.9 hours. The system was agitated and resulted in a temperature peak occurring after 24.4 hours for a total induction time of 21.5 hours. After an experimental run of 72.4 hours, the system ended at 319 psig. The calculated water removal by hydrate formation is 5.7 wt% to 12.8 wt%. In a system with excess carbon dioxide gas, the theoretical water removal by hydrate formation is estimated to be 5.6 wt% to 12.6 wt%. In a system with excess water, the theoretical water removal by hydrate formation is estimated to be 9.7 wt% to 22.0 wt%.

4.6 Determination of Hydrate Formation

Hydrate formation was confirmed by plotting the reactor pressure, reactor temperature, and bath temperature data versus time. Clathrate hydrate formation results in a spike in temperature followed by a drop in pressure. By plotting this data, visual confirmation of hydrate formation can be confirmed. Figure 4.2 is an example of these graphs, showing the experimental data for Run 4. A large temperature spike can be seen on the graph followed by a pressure drop, signifying hydrate formation.

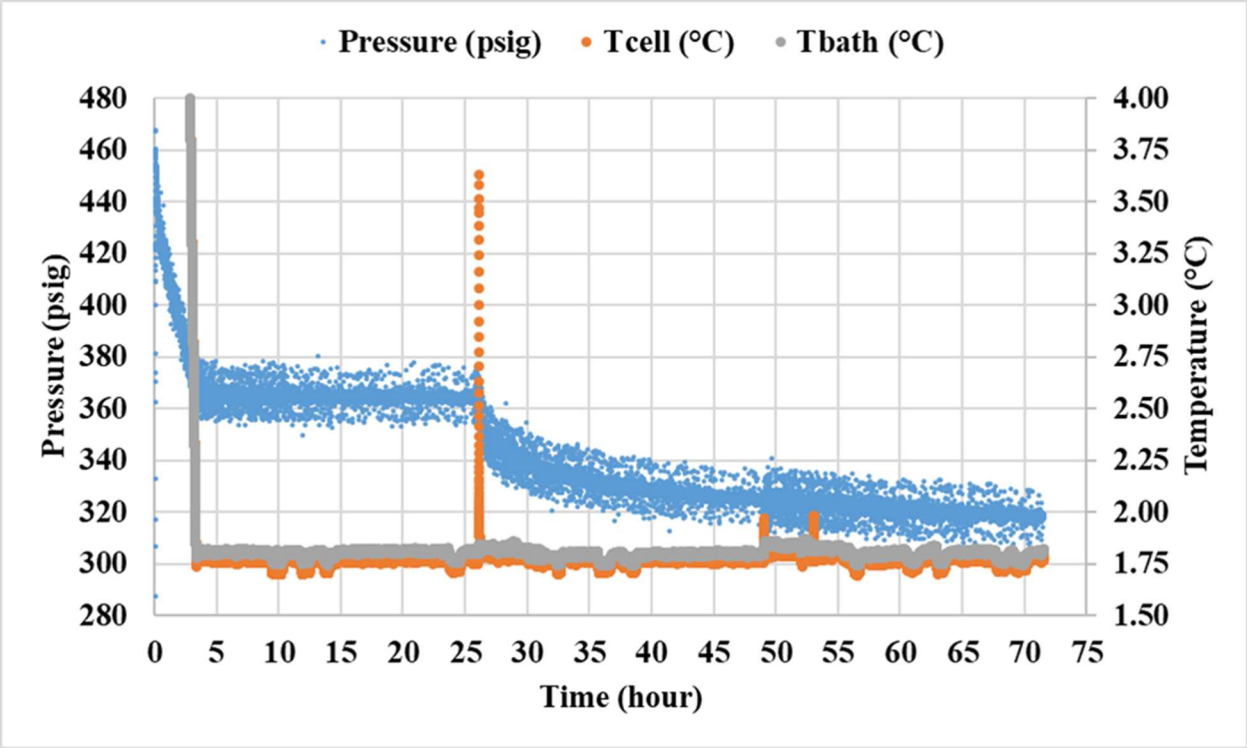

Figure 4.2 – Run 4 Experimental Data

Due to a large amount of data and electronic noise from equipment, graphs for experimental runs were refined. The first step of refining the data was collecting every 6th point. This was performed with the INDEX function in excel by using =@INDEX(Data Range, ROWS(3:$3)*6-5). This function would remove the last 5 data points in a set of 6 points. After refining the time, pressure, and temperature data of an experimental run with this method, a median smoothing would be applied to reduce noise. For pressure and temperature, the median of 5 points would be taken at the resulting time intervals. This reduced the number of peaks from noise significantly. Figure 4.3 is Run 4's experimental data that underwent this refining process. In obtaining a smoother curve with less noise, the temperature peak is at a smaller magnitude than previously. Small peaks from later agitation are additionally less noticeable.

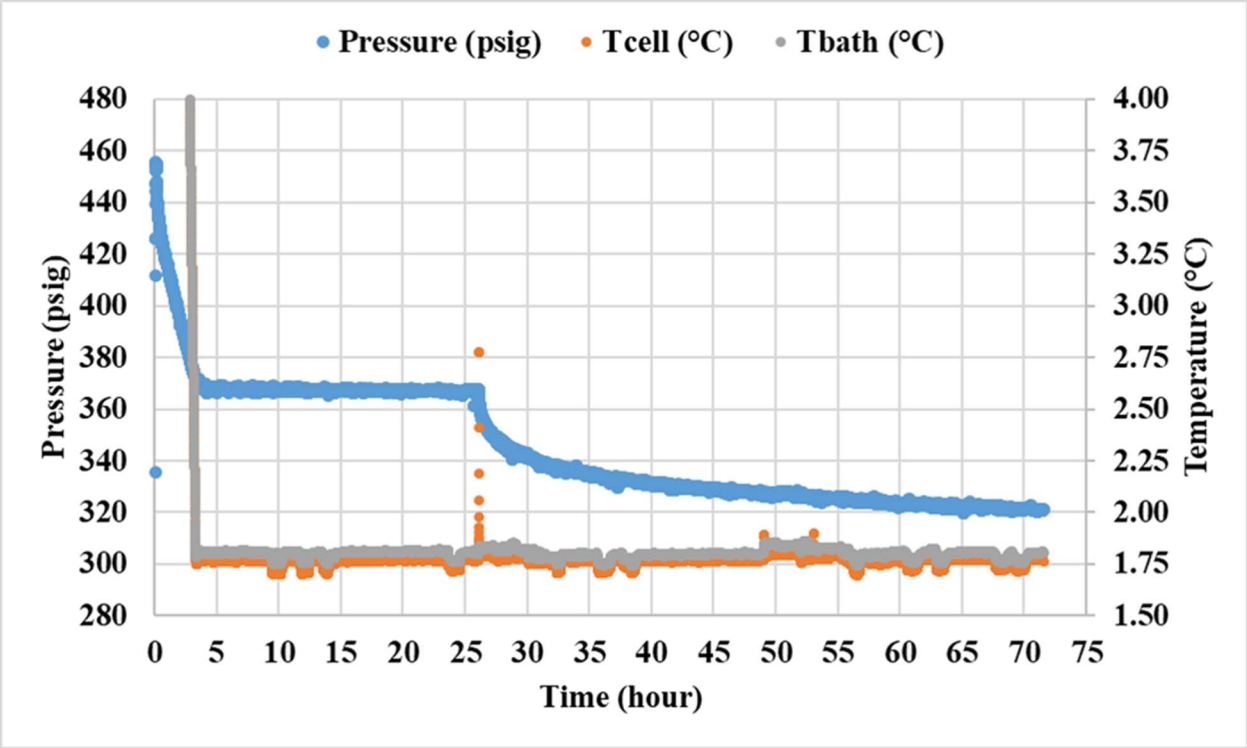

Figure 4.3 – Run 4 Experimental Data Refined

4.7 Dissociation and Carbon Dioxide Hydrate Equilibrium

Dissociation was used to collect pressure and temperature data to determine if there was carbon dioxide hydrate equilibrium in algal growth medium and algal solutions. The presence of pressure-temperature equilibrium in the solution would confirm the formation of carbon dioxide hydrates during the experimental run. To collect data to confirm if equilibrium occured, the pressure was gradually dropped in steps which resulted in temperature decreasing. The length of steps varied by how long it took for the temperature to return to the starting temperature. The length of steps also varied due to dissociation requiring two researchers to operate the process; one to track the pressure drop and one to release pressure from the three-way valve. As a result, time varied, but all dissociation experiments were stochastic. To help signify these steps, a color was assigned for both temperature and pressure for every step. Thus, when looking at a graph from

Run 1 and Run 4, step 4 would have the same color graphically. The color-coding of steps for dissociation can be seen for Run 4 in Figure 4.4.

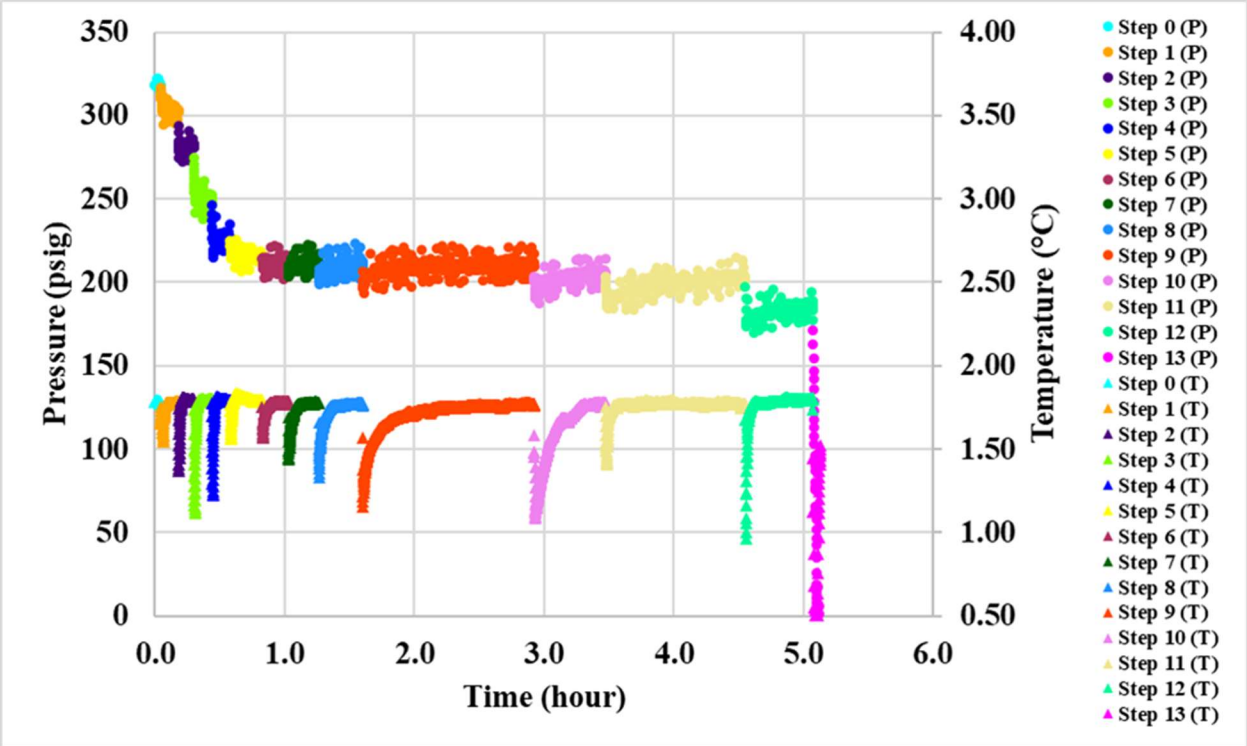

Figure 4.4 – Run 4 Dissociation

From the dissociation data, the temperature and pressure of the reactor are important to plot the pressure-temperature equilibrium curves of carbon dioxide hydrate formation. For these plots, the pressure is plotted versus temperature. Steps in these graphs use similar color-coding processes to relate the steps in dissociation. For equilibrium, not all dissociation steps are relevant. Typically steps where the temperature does not increase to the original temperature quickly contribute to equilibrium data. Steps where the pressure slowly increases typically contribute to equilibrium data, as the system tries to maintain hydrate equilibrium after a pressure decrease. These steps will typically approach or attempt to approach 210 to 212 psig. Figure 4.5 shows the full potential equilibrium data for Run 4. As seen, some steps do not contribute to the equilibrium data. Known equilibrium curves are additionally plotted.

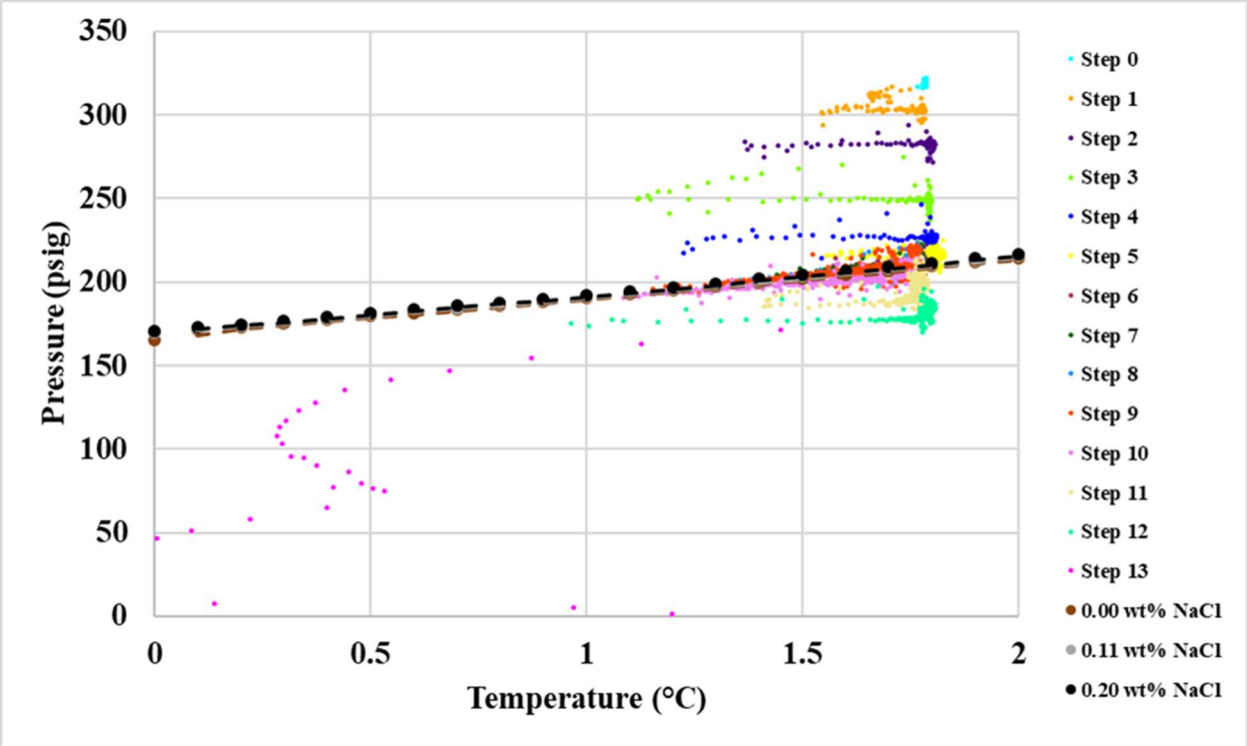

Figure 4.5 – Run 4 Equilibrium

With these considerations, determining which steps contribute to equilibrium data via graphic representation can be utilized to filter data. Each step was analyzed graphically to see if pressure increases as temperature increases. In dissociation steps where temperature returns quickly to the bath temperature, the pressure typically does not vary significantly with temperature. As a result, these steps can be excluded from the equilibrium data. Steps with pressure significantly higher or lower than 210 to 212 psig were excluded from equilibrium data. Most equilibrium data determined from experimental dissociation occurred from 1.0°C to 1.8°C. From 1.0°C to 1.8°C, the equilibrium pressure for carbon dioxide hydrates ranges from approximately 190 psig to 215 psig. These considerations can aid in graphically eliminating steps that might not be relevant by reducing the boundaries of the graph to these values. Figure 4.6 shows this methodology applied to the equilibrium data collected from Run 4's Dissociation.

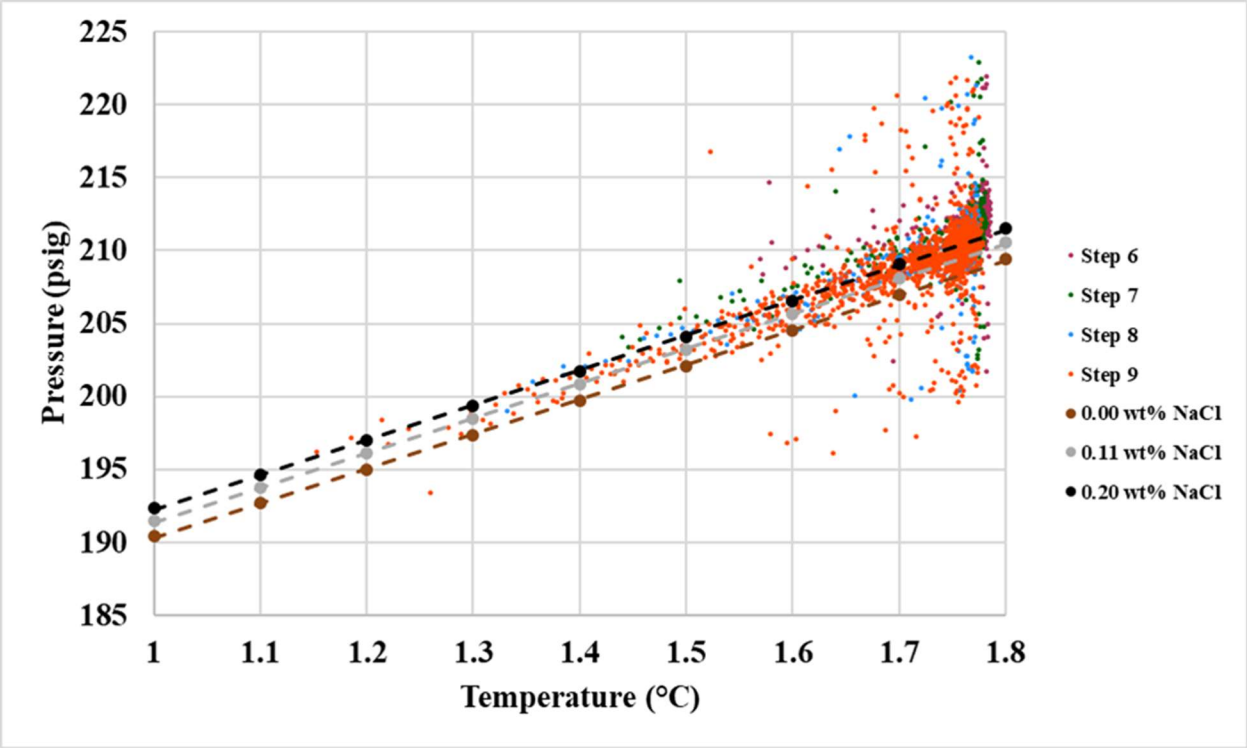

Figure 4.6 – Run 4 Equilibrium After Step Elimination

Chapter 5: DISCUSSION

5.1 Carbon Dioxide Hydrates

5.1.1 Formation in Algal Solutions and Growth Media

Carbon dioxide hydrates can form in algal solutions and growth media; however, this formation requires agitation of the system. All graphs used to graphical confirm hydrate formation can be found in the Appendix. Experimental Run 5 was used to find the induction time of carbon dioxide hydrate formation that occurs independently of agitation. However, after waiting approximately a week, signs of formation still had not occurred and the system was agitated to encourage the formation of carbon dioxide hydrates. As with all experiments, hydrate formation occurred within 30 minutes after this agitation. If this methodology is to be used for large volume algal solution dewatering, the system would require technology or operators to agitate the system. The requirement of agitation to encourage hydrate formation can potentially limit the application of this methodology of dewatering algal solutions as a result. Mechanical agitation could be performed by a shaking table to emulate the agitation performed by operators in this study. The use of stirring may be an alternative; however, this study did not use a system that utilized stirring for agitation. Developing a dewatering system that can mechanically agitate the system may not be economically feasible. Further, having operators agitate large volume algal solutions under moderately high pressure manually may provide unsafe working conditions.

5.1.2 Dewatering of Algal Solutions and Growth Media

A summary of experimental and theoretical dewatering results can be found in Table 5.1. The minimum experimental water uptake by hydrate formation was typically slightly higher than the minimum theoretical water uptake from hydrate formation under excess gas conditions and

less than the minimum theoretical water uptake from hydrate formation under excess water conditions. The maximum experimental water uptake by hydrate formation was typically higher than the maximum water uptake by hydrate formation under excess gas conditions and significantly lower than the maximum theoretical water uptake by hydrate formation under excess water conditions. Based on these results, the system condition was likely excess carbon dioxide gas, meaning more carbon dioxide gas was added to the system than can be used by hydrate formation. The maximum experimental values are not achievable as there is pressure drop from solubility in this system. The extent of this pressure drop in this study can only be estimated theoretically to a maximum pressure drop which may not reflect the actual pressure drop from carbon dioxide solubility. When the system is first pressurized, the system is agitated to allow for the pressure drop from the solubility of the carbon dioxide at the start of the experiment and then pressurized again. As a result, the solution at the start of the experiment can be assumed to be partially full of solubilized carbon dioxide. As the temperature drops, the solubility of carbon dioxide in the solution will increase, but less carbon dioxide will dissolve than if the system was not agitated at the start of the experiment. During the time in which the pressure approaches the flatline temperature, carbon dioxide likely dissolves into the solution as it does at the start of the experiment. Thus, during the pressure drop from the flatline pressure to the final pressure, there will be some pressure drop from solubility, but it will not play a significant role. It can thus be assumed, the actual water uptake of water from hydrate formation is within the range of theoretical water uptake by hydrate formation under excess carbon dioxide.

Table 5.1 – Experimental and Theoretical Water Uptake by Hydrate Formation

Run Order	Solution	Experimental		Theoretical			
				Excess Gas		Excess Water	
		Water Uptake%		Water Uptake%		Water Uptake%	
		Min	Max	Min	Max	Min	Max
1	*Chlorella* subculture	0.2%	8.0%	0.2%	7.6%	0.4%	13.5%
2	Alga-Gro	1.8%	9.4%	1.7%	9.3%	3.1%	16.4%
3	*Chlorella* subculture	5.1%	12.9%	4.9%	12.3%	8.6%	21.7%
4	Alga-Gro	4.2%	12.0%	4.2%	11.9%	7.4%	21.0%
5	*Chlorella* subculture	4.1%	11.5%	3.9%	10.9%	6.8%	19.0%
6	Concentrated *Chlorella*	7.3%	14.7%	7.4%	14.5%	12.9%	25.3%
7	Concentrated *Chlorella*	1.9%	8.7%	1.9%	8.5%	3.3%	14.9%
8	Concentrated *Chlorella*	5.7%	12.8%	5.6%	12.6%	9.7%	22.0%

5.1.3 Growth Media Unknowns

The chemical composition of Carolina® Alga-Gro Medium was unable to be obtained. As a result, the chemical composition of the growth medium is relatively unknown. Based on public growth solution compositions, salts are commonly used to provide algae with minerals and trace elements for growth. Most salts used in the algae growth medium contain sodium, potassium, magnesium, and calcium. Nitrogen and phosphorus are also included in growth mediums due to the importance of growing plants. Trace elements can include metals such as iron. As a result, it can be concluded that the growth medium and subcultures using this growth medium contained some concentration of salts, though which exact salts are unknown.

UTEX Proteose Medium is a modified Bristol Medium that was used to seed the UTEX 2714 *Chlorella vulgaris*. Bristol Medium uses six salts in its growth media. These salts are sodium nitrate, calcium chloride, magnesium sulfate, dipotassium phosphate, potassium dihydrogen phosphate, and sodium chloride (The University of Texas at Austin, (n.d.)). The Walne Medium is another freshwater algal growth media. This media is more complex than the Bristol Medium.

The salts used in the Walne Medium are ferric chloride, manganous chloride, disodium salt, sodium dihydrogen orthophosphate, sodium nitrate, zinc chloride, cobaltous chloride, cupric sulfate, and sodium metasilicate (Food and Agriculture Organization of the United Nations, (n.d.)). The National Center for Marine Algae and Microbiota (n.d.) provides compositions for several freshwater and saltwater algal growth mediums. Two general freshwater algae growth mediums are the AF6 Medium and MES Volvox Medium. The AF6 Medium uses sodium nitrate, magnesium sulfate, dipotassium phosphate, potassium dihydrogen phosphate, and calcium chloride as salts in its growth medium. The MES Volvox Medium uses calcium nitrate, magnesium sulfate, and potassium chloride as salts in its growth medium. With most freshwater algae growth mediums potassium, magnesium, and calcium salts are used. Sodium and trace metal salts also are used but vary by growth medium.

5.1.4 Pressure-Temperature Equilibrium

The manual selection of steps was the methodology selected for plotting pressure-temperature equilibrium for each experimental run. Pressure-temperature graphs for each experimental run can be found in the Appendix. All pressure-temperature data used to plot equilibrium was collected from dissociation. To find potential trends in pressure-temperature equilibrium for each solution, graphs were created using each experimental run. These graphs used data from the selected dissociation steps for each experimental run plotted as one series.

Figure 5.1 shows the pressure-temperature equilibrium for the control experiments which only used Carolina® Alga-Gro Freshwater Medium. Experimental data from Steps 6 and 7 were used for Run 2 and Steps 6, 7, 8, and 9 were used for Run 4. Known pressure-temperature equilibrium curves for water containing 0.00 wt% sodium chloride, 0.11 wt% sodium, and 0.20 wt% sodium were additionally plotted. Salt can inhibit the formation of hydrate formation,

resulting in higher equilibrium pressures. The media solutions were ultimately unknown, thus based on known algal growth media solutions salts may be present. The first observation from Figure 5.1 is that Run 2 and Run 4 have a similar pressure-temperature equilibrium data cloud. Minor differences may be present, but similar trends present show the experimental runs are stochastic. Further, this set of data appears to be similar to a pressure-temperature equilibrium curve of water containing salt. The experimental data is primarily higher pressures than pure water as temperature increases. Pressures are more like pressure values from the equilibrium curve of water containing 0.20 wt% sodium chloride.

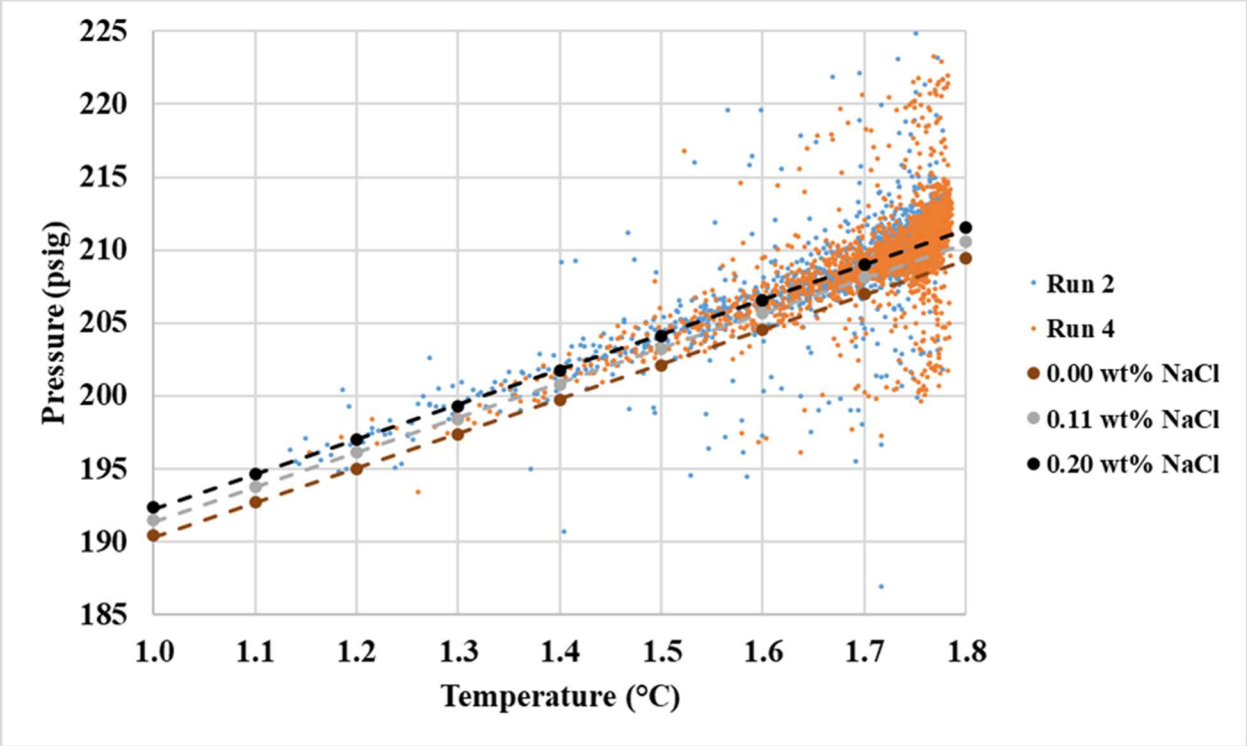

Figure 5.1 – Carolina® Alga-Gro Medium Pressure-Temperature Equilibrium

Figure 5.2 shows the pressure-temperature equilibrium for experiments that used an algal solution from the CAROLINA™ 15-3068 Concentrated *Chlorella* subculture. Experimental data from Steps 6, 7, 8, 9, and 10 were used for Runs 1 and 3 and from Steps 7, 8, 9, and 10 for Run 5. Though Run 5 had a significantly longer run time, the dissociation process took a similar length

of time as all other experimental runs. Runs 1, 3, and 5 all produced similar sets of pressure-temperature data. These experimental run data sets do vary slightly than data sets produced by Runs 2 and 4. As temperature increases, pressure appears to be greater than values from the pressure-temperature equilibrium curve of pure water, however, some pressure values do vary around that equilibrium curve. Due to noise and other factors, a clear curve cannot be determined, but the cloud created by the data seems to closest match the water containing 0.11 wt% sodium chloride equilibrium curve.

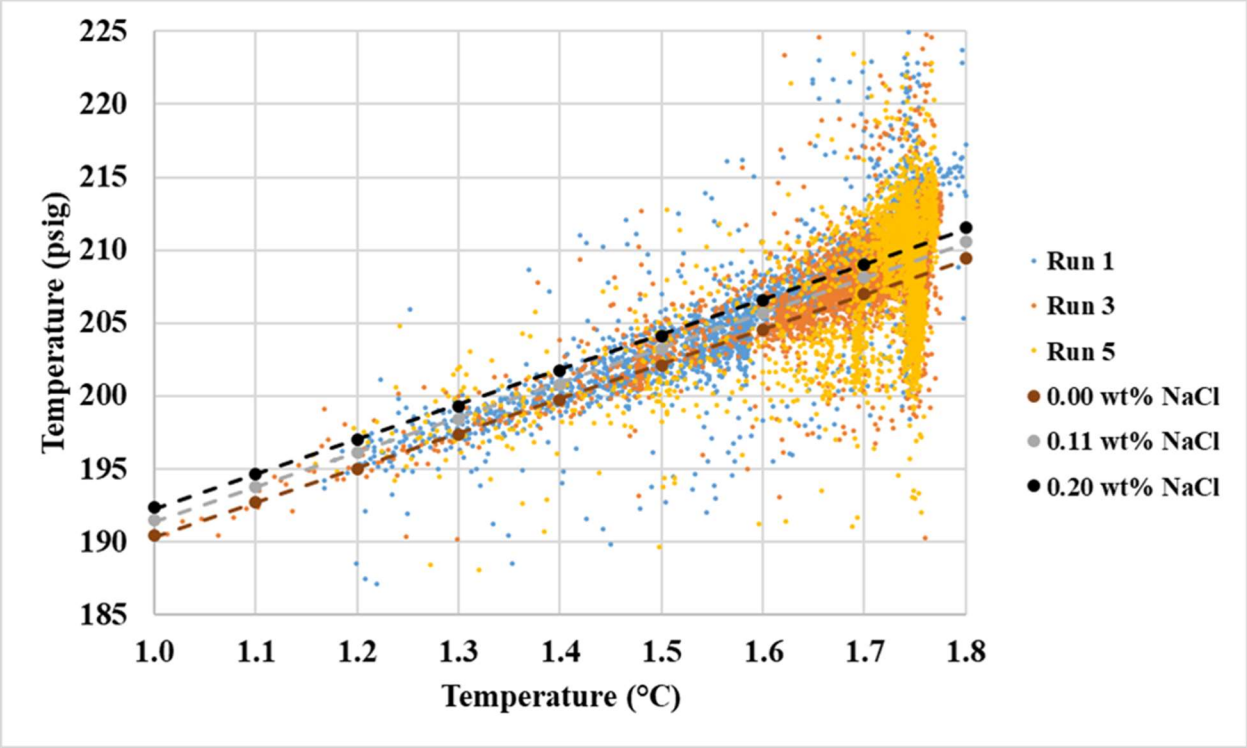

Figure 5.2 – CAROLINA™ 15-3068 Concentrated Chlorella Subculture Pressure-Temperature Equilibrium

Figure 5.3 shows the pressure-temperature equilibrium for the control experiments which only used an algal solution from the CAROLINA™ 15-3068 Concentrated *Chlorella* culture. Experimental data from Steps 6, 7, 8, and 9 were used for Runs 6 and 8 and from Steps 7, 8, 9, and 10 for Run 7. Runs 6, 7, and 8 all produced similar sets of pressure-temperature data. These data

sets do vary slightly than data sets produced by Runs 1 through 5. As temperature increases, pressure appears to be greater than values from the pressure-temperature equilibrium curve of pure water. Additionally, most steps appear to have pressure higher than the equilibrium pressure of water containing 0.20 wt% sodium chloride as temperature increases. This was seen slightly with data sets created by Runs 1, 3, and 5. Some experimental equilibrium pressure data points are less than the equilibrium values of water containing 0.20 wt% sodium chloride as temperature increases, however, most are not. Due to noise, a clear curve cannot be determined, but the cloud created by the data seems to primarily like an equilibrium curve with a higher weight percentage of salt.

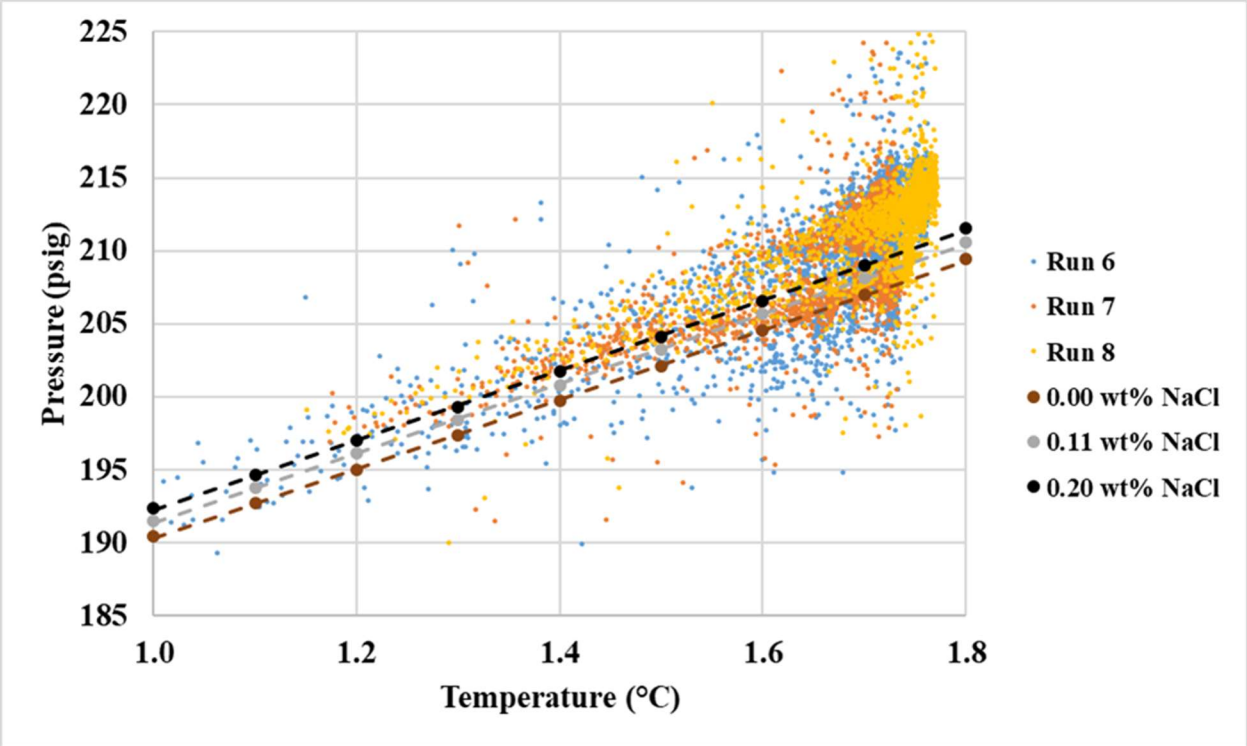

Figure 5.3 – CAROLINA™ 15-3068 Concentrated Chlorella Culture Pressure-Temperature Equilibrium

Ultimately this data shows that each solution has a unique impact on equilibrium pressure. This impact is similar to the impact that salts have on the equilibrium pressure of carbon dioxide

hydrates in water. The increase in equilibrium pressure may be tied to a solution's concentration of algae. The control experimental runs used Carolina® Alga-Gro Medium which, likely due to unknown salts, had temperature-equilibrium data similar which varied around the equilibrium curve of water containing 0.20 wt% sodium chloride. Though noise varied greater with pressure-temperature equilibrium data from experimental runs using an algal solution from the CAROLINA™ 15-3068 Concentrated Chlorella subculture, many experimental equilibrium pressure values were higher than plotted known equilibrium curves. The algal solution from the CAROLINA™ 15-3068 Concentrated Chlorella culture had a higher algae concentration than its subculture. The equilibrium data from runs using an algae solution from the CAROLINA™ 15-3068 Concentrated *Chlorella* culture have more equilibrium pressure values higher than plotted known equilibrium curves than the equilibrium pressure values from its subculture. Further, unlike its subculture, equilibrium pressure values rarely were less than the pressure-temperature equilibrium curve of pure water.

5.2 Impact of Experimental Conditions on Algal Solution

The survival of algae is important for the extraction of oils. An algal solution is usually dewatered until dry; the destruction of algal cells is to be avoided to extract as much oil from the algal biomass as possible. As a result, it is important for an algal dewatering process to not damage algal cells or kill algae before biomass can be created and the oil extracted. For the process of using carbon dioxide hydrate formation to dewater an algal solution, the algae have an approximate three-day survival timespan after being removed from the reactor. A comparison of algal solutions after experiments can be seen in Figure 5.4 Algae removed from the reactor after an experiment typically died after three days and would not grow when reseeded in a new algal growth medium.

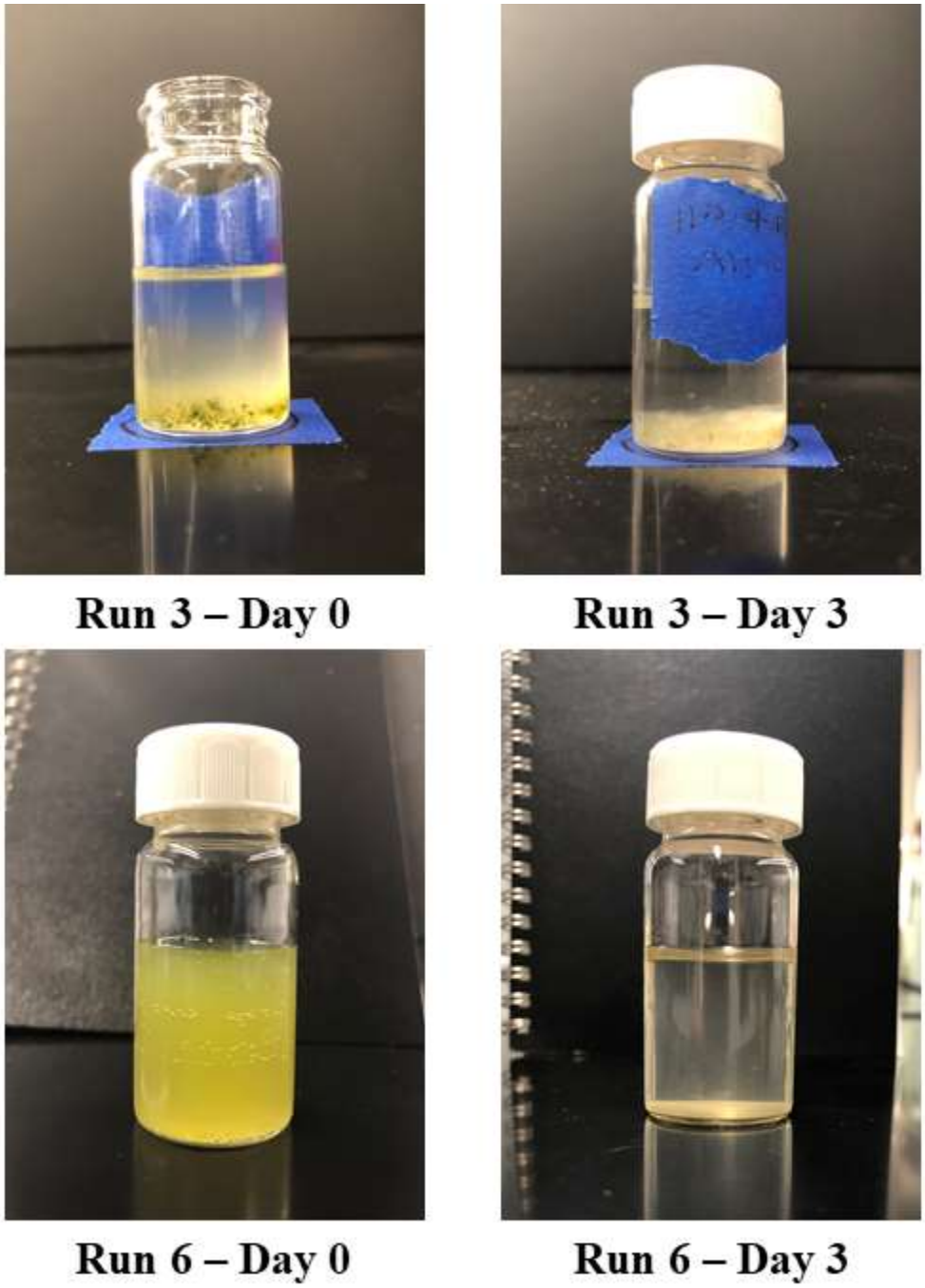

Figure 5.4 – Algae Collected After Experimental Runs

It is unconfirmed which experimental conditions contribute to the eventual death of the algae. Operating temperatures are significantly lower than ideal growing conditions, and the algae do not get light in the reactor. The Food and Agriculture Organization of the United Nations (n.d.)

reports the optimal growth temperature for algae is 18 to 24°C with a light intensity of 2,500 to 5,000 lux for at least 16 hours. The temperature of the reactor is significantly less than the optimum growth conditions and has a light intensity of 0 lux. The reactor atmosphere is primarily carbon dioxide as carbon dioxide is used to pressurize and fill the reactor. *Chlorella* has been grown in conditions with atmospheres containing higher concentrations of carbon dioxide than standard air. A study by Hanagata et al. (1992) found Chlorella sp. had a maximum carbon dioxide atmospheric concentration tolerance of 40%. A study by Sung et al. (1999) found good growth conditions for *Chlorella* sp. grown in an environment with an atmospheric carbon dioxide concentration of 30%. The concentration of carbon dioxide in the reactor's atmosphere likely greatly exceeds these conditions. It can be assumed all three of the experimental conditions contribute to the eventual death of algae, however, this study has not tested growing *Chlorella* in conditions that emulate these conditions.

The lifespan of the algae after hydrate formation occurs must be considered if plans to utilize this method of dewatering are used. If this methodology is used as a primary dewatering process, further dewatering of oil extraction would need to occur shortly after the algae is removed from the reactor to ensure the most algae survives. This can place further technical and economic infeasibility on this methodology as it may not be technically possible to extract oil from the algae on the same day. Costs associated with the loss of some algae may additionally add up as large volumes of algae are used.

5.3 Future Studies

5.3.1 Induction Time

Future studies can be performed to optimize induction time. The agitation of the system resulted in the encouragement of algae hydrate formation. The agitation of the system typically occurred shortly before the time of the first temperature peak which resulted in a pressure drop. The reactor system was typically agitated the next day after the system was setup. Future studies can attempt to find the shortest induction time by agitating the system in set periods after the reactor reaches the flatline temperature. This can be done for several different time-lapses until the shortest induction time is found. Future studies focusing on induction time can additionally try other forms of agitation. In this study, just manual agitation by an operator was performed. The use of a mechanical shaking table could potentially be used. The use of stirring could additionally be studied to see if continuous agitation impacts the induction time.

5.3.2 Step Standardization

Depressurization of the reactor required two operators; one to open the three-way valve and one to track the pressure drop. The length of steps in experimental dissociation runs varied due to restrictions related to the need of two operators. If an operator was not available, the reactor could not be depressurized. Future studies should attempt to standardization the time steps are allotted. By each step being the same length of time, a similar amount of pressure and temperature data can be collected. Further, time steps can be designed based on the length of long steps to minimize steady-state data. This can likely provide pressure-temperature equilibrium data that is less noisy.

5.3.3 Dewatering Algal Solutions as a Secondary Process

For this study, dewatering of algal solutions with carbon dioxide hydrate formation was performed as a primary dewatering process. Primary dewatering processes typically attempt to remove as much bulk water as possible. Due to the amount of water removed by this dewatering process, carbon dioxide hydrate formation would not make a good primary dewatering process. Future studies should try an algal solution that has undergone a feasible primary dewatering process such as filtration. Future studies can utilize the CAROLINA™ 15-3068 Concentrated Chlorella culture for this effectively. Each vial of this solution is sold at a standard of 60 mL and throughout several hours' algae settles. Removing water once algae have settled via pipetting can act as a primary process before the algal solution is used can emulate a primary dewatering process.

5.3.4 Operation Costs

Operating costs were not calculated in this study; however, economic feasibility is assumed to be low when compared to other dewatering processes. The process of dewatering algal solutions with carbon dioxide requires large amounts of energy for cooling the reactor and complex pressurized systems when compared to a process such as the use of a centrifuge. Future studies can look at a more accurate economic feasibility of this dewatering process.

Chapter 6: CONCLUSIONS

The research conducted by this study has the following conclusions:

- Carbon dioxide hydrates can form in algal growth mediums and algal solutions
    - Agitation is required to encourage this formation
    - All experimental runs showed pressure decline after temperature spiked in the reactor after agitation, indicating the presence of gas hydrates
- The formation of carbon dioxide hydrates can dewater algal solutions
    - This study found overall 0.2 to 14.7 wt% of free water in algal solutions was converted into clathrate hydrates
    - This study found overall 1.8 to 12.0 wt% of free water in algal growth media was converted into clathrate hydrates
- The calculated experimental free water conversion suggests the system in this study was under excess gas conditions
    - The range of theoretical weight% of free water converted into clathrate hydrates calculated are close to experimental free water conversion ranges
    - Differences in the maximum values of these ranges can be explained by the presence of a pressure drop due carbon dioxide solubility
- Pressure-temperature equilibrium for carbon dioxide hydrates in algal growth media and algal solutions typically had higher pressures than the pressure-temperature equilibrium of carbon dioxide hydrates in pure water
    - Pressure-temperature equilibrium of carbon dioxide hydrates in water containing salts fits data, suggesting the presence of salts used in algal growth media and algal solutions impacts the pressure-temperature equilibrium

APPENDIX

Appendix A: Hydrate Formation of Experimental Runs

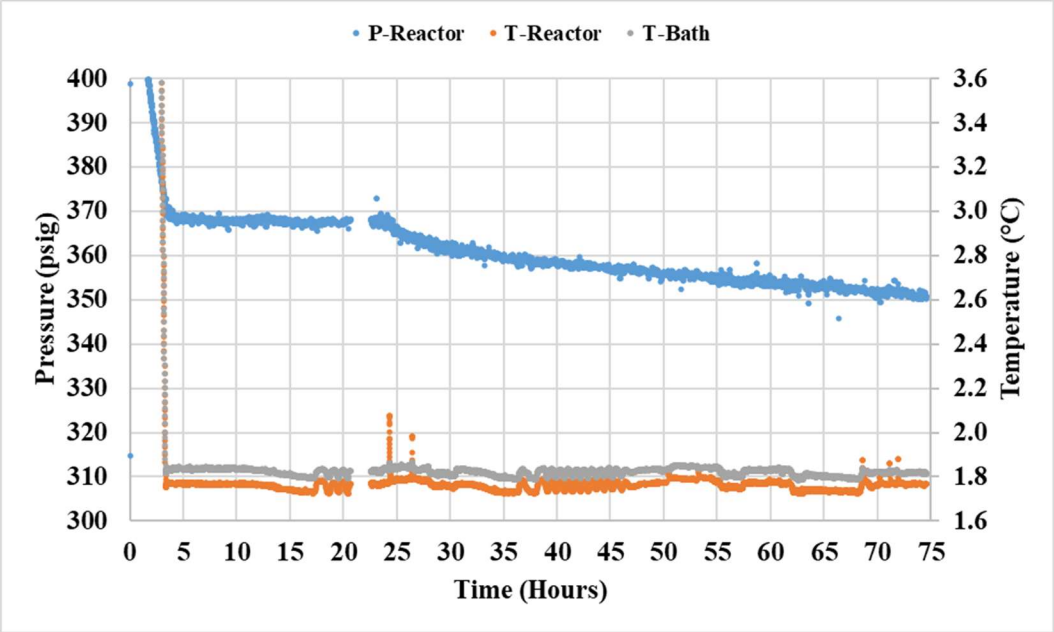

Figure A.1 – Experimental Run 1 Hydrate Formation

Temperature spike occurring at approximately 24.3 hours can be seen on the T-Reactor series. After this temperature spike, the pressure decreased as seen by the P-Reactor series.

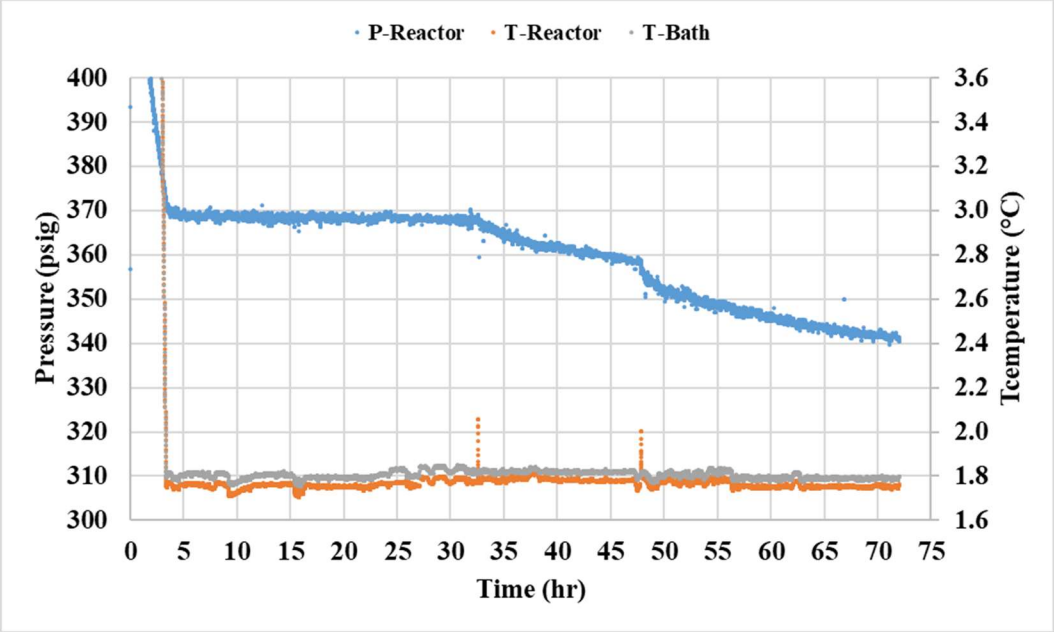

Figure A.2 – Experimental Run 2 Hydrate Formation

Temperature spike occurring at approximately 32.6 hours can be seen on the T-Reactor series. After this temperature spike, the pressure decreased as seen by the P-Reactor series.

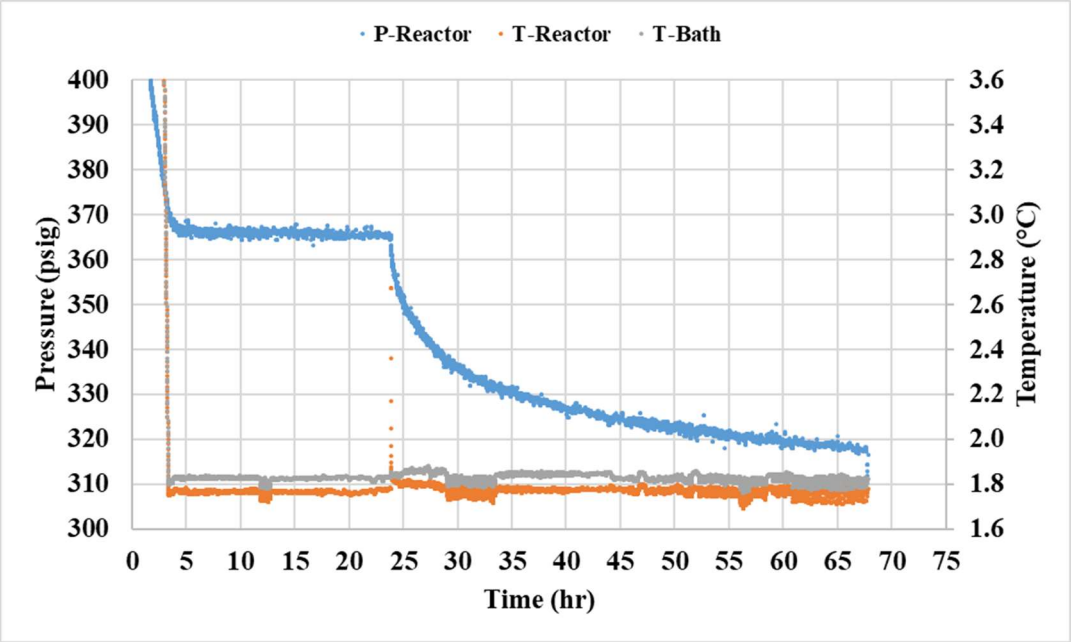

Figure A.3 – Experimental Run 3 Hydrate Formation

Temperature spike occurring at approximately 33.8 hours can be seen on the T-Reactor series. After this temperature spike, the pressure decreased as seen by the P-Reactor series.

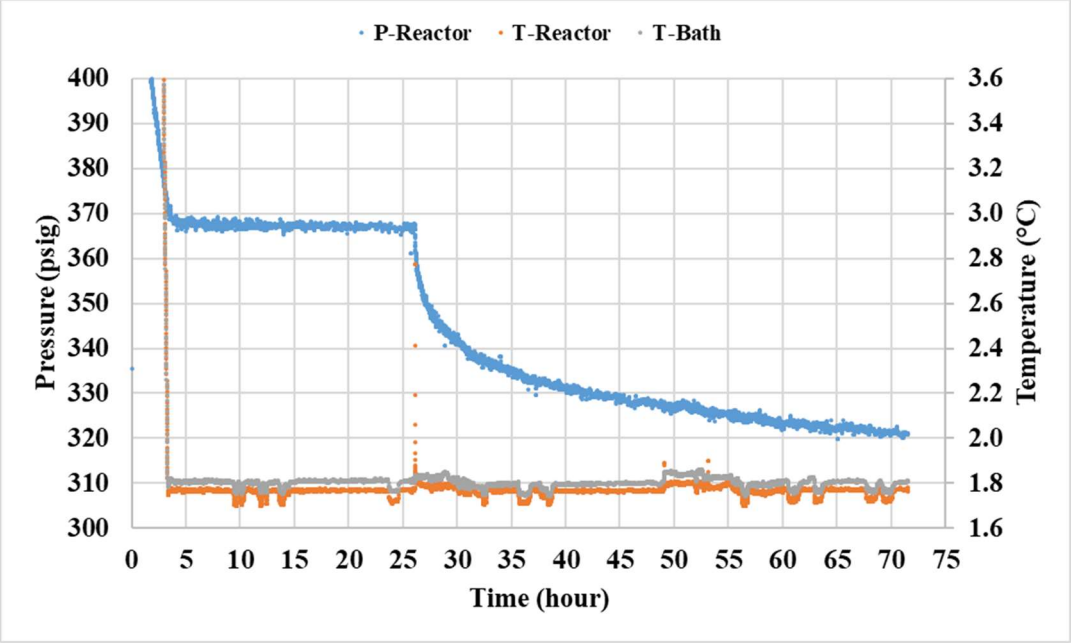

Figure A.4 – Experimental Run 4 Hydrate Formation

Temperature spike occurring at approximately 26.1 hours can be seen on the T-Reactor series. After this temperature spike, the pressure decreased as seen by the P-Reactor series.

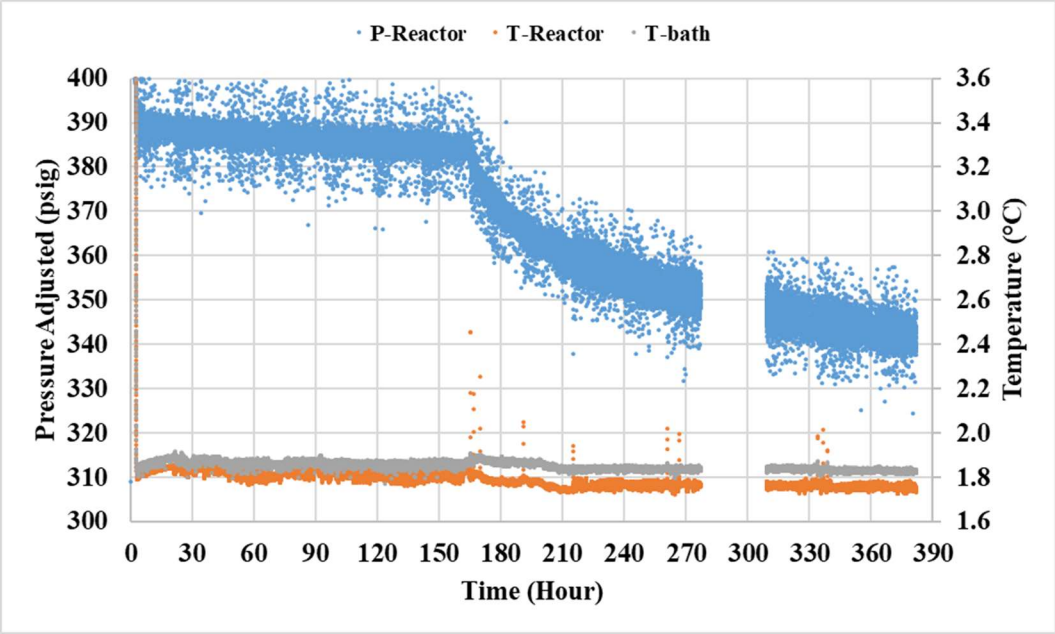

Figure A.5 – Experimental Run 5 Hydrate Formation

Temperature spike occurring at approximately 165.1 hours can be seen on the T-Reactor series. After this temperature spike, the pressure decreased as seen by the P-Reactor series.

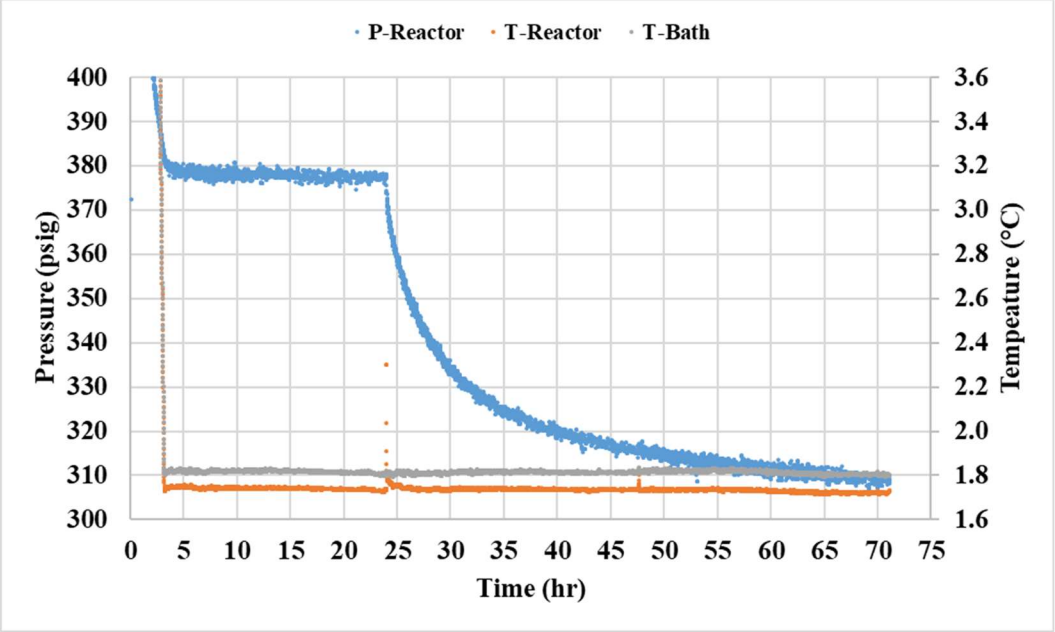

Figure A.6 – Experimental Run 6 Hydrate Formation

Temperature spike occurring at approximately 24.0 hours can be seen on the T-Reactor series. After this temperature spike, the pressure decreased as seen by the P-Reactor series.

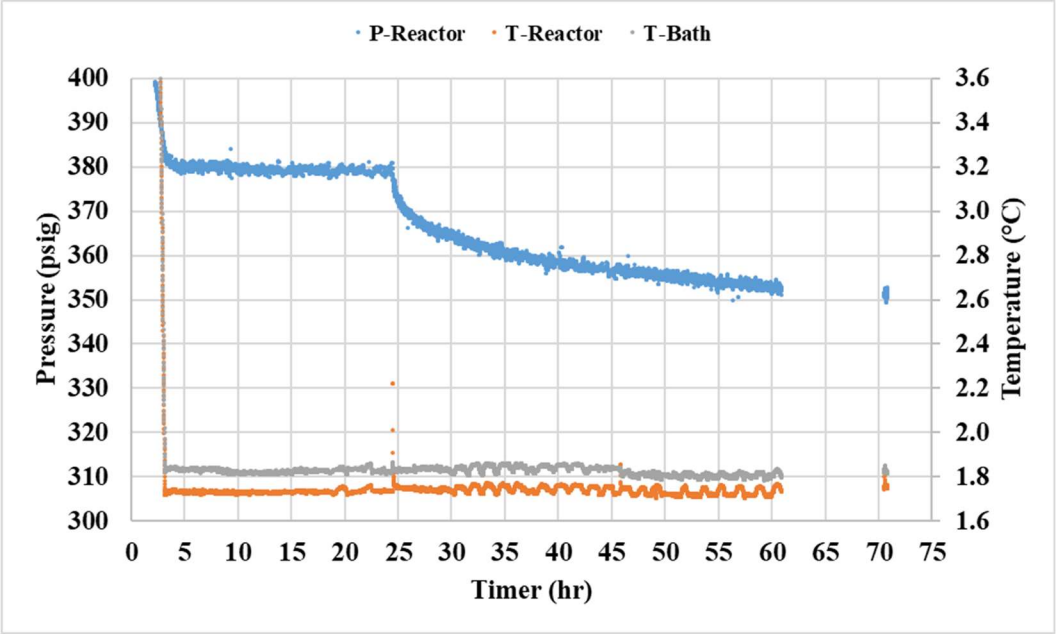

Figure A.7 – Experimental Run 7 Hydrate Formation

Temperature spike occurring at approximately 24.5 hours can be seen on the T-Reactor series. After this temperature spike, the pressure decreased as seen by the P-Reactor series.

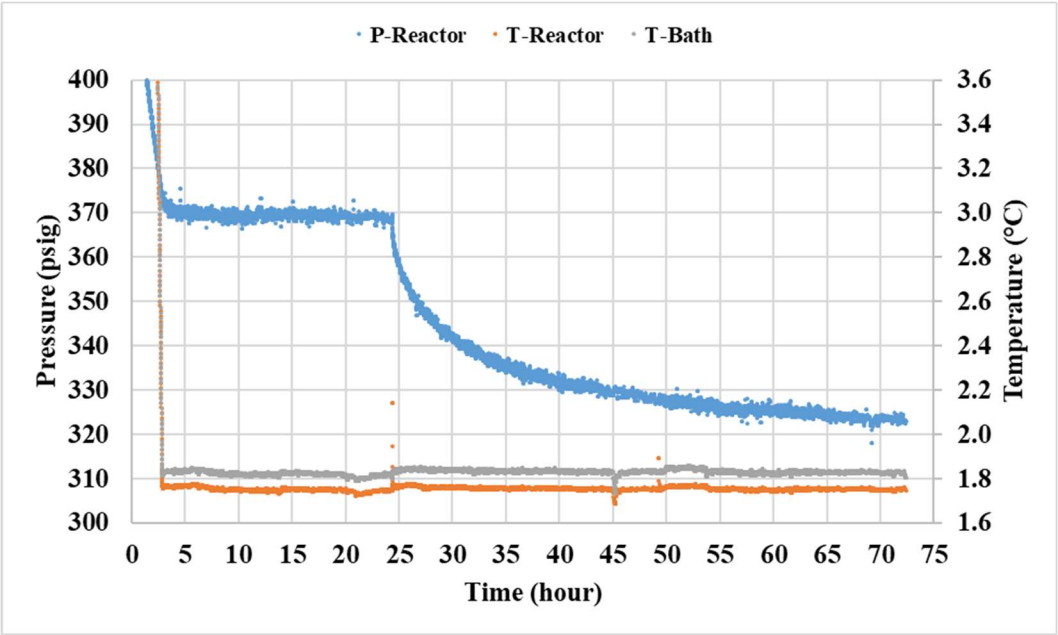

Figure A.8 – Experimental Run 8 Hydrate Formation

Temperature spike occurring at approximately 24.4 hours can be seen on the T-Reactor series. After this temperature spike, the pressure decreased as seen by the P-Reactor series.

Appendix B: Pressure-Temperature Equilibrium

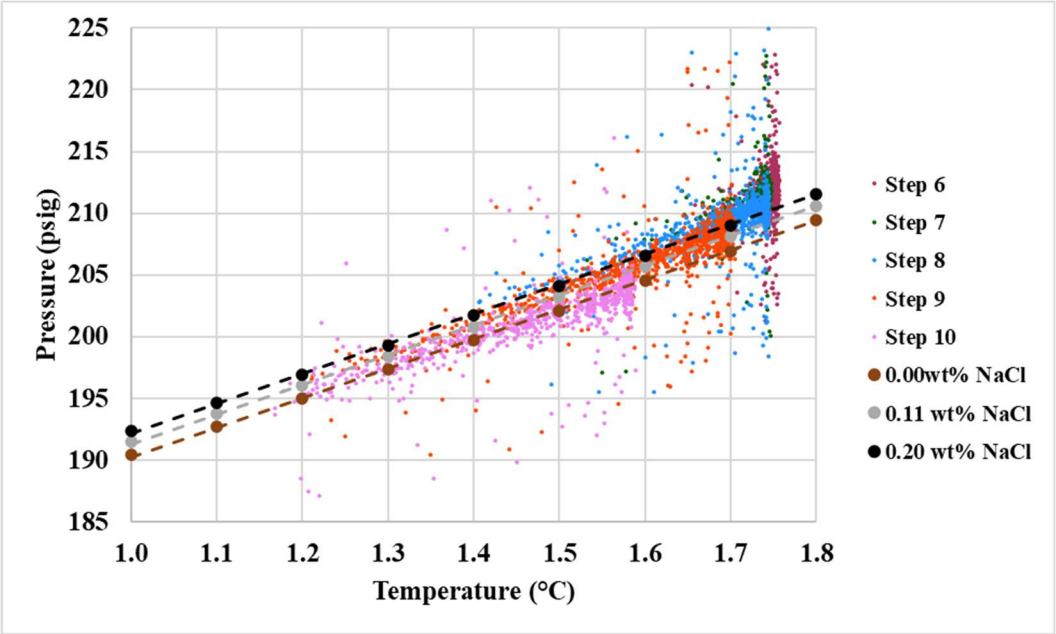

Figure B.1 – Experimental Run 1 Pressure-Temperature Equilibrium

Steps 6 through 10 were plotted for the pressure-temperature data of this experimental run. Known pressure-temperature curves of carbon dioxide hydrates were additionally plotted.

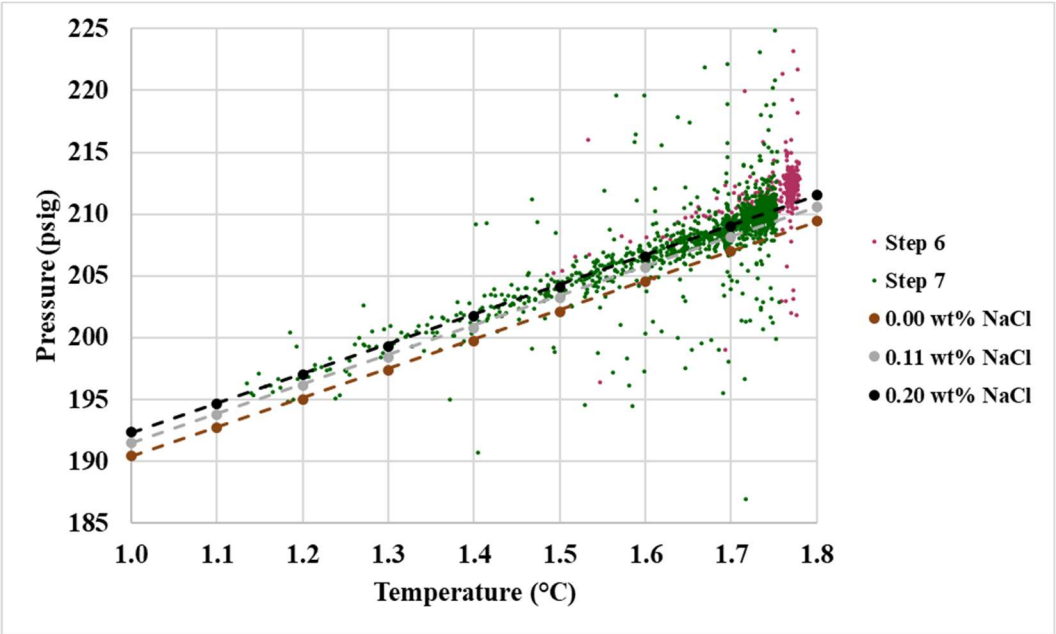

Figure B.2 – Experimental Run 2 Pressure-Temperature Equilibrium

Steps 6 through 7 were plotted for the pressure-temperature data of this experimental run. Known pressure-temperature curves of carbon dioxide hydrates were additionally plotted.

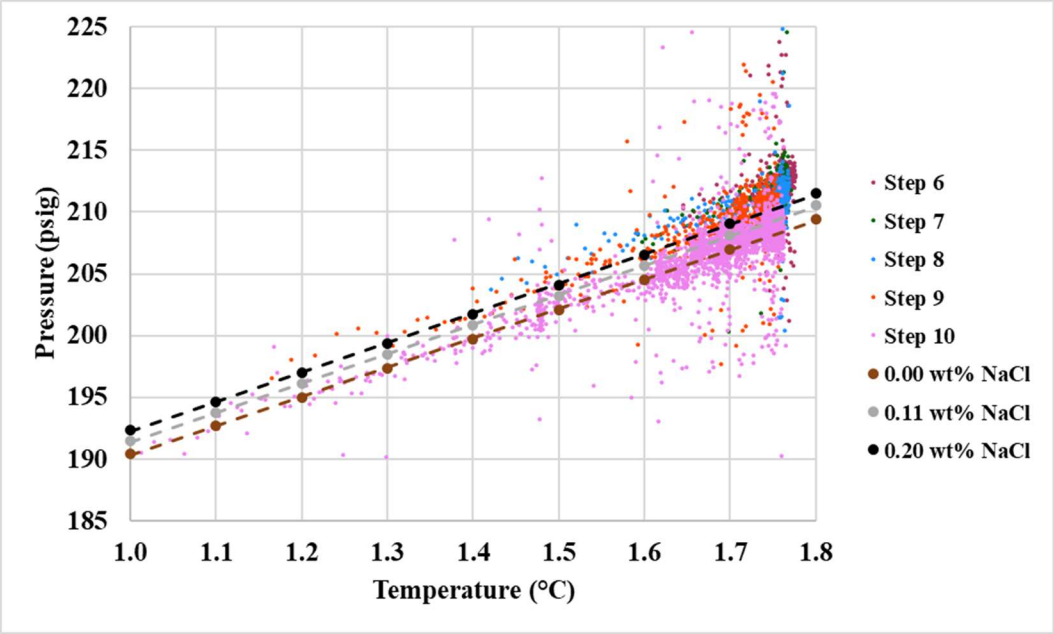

Figure B.3 – Experimental Run 3 Pressure-Temperature Equilibrium

Steps 6 through 10 were plotted for the pressure-temperature data of this experimental run. Known pressure-temperature curves of carbon dioxide hydrates were additionally plotted.

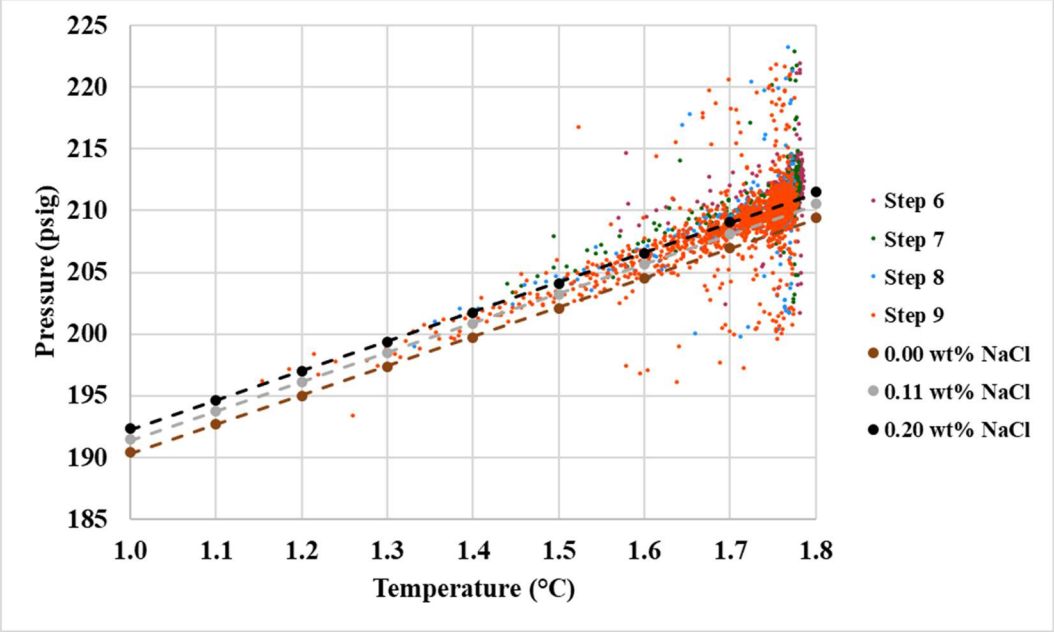

Figure B.4 – Experimental Run 4 Pressure-Temperature Equilibrium

Steps 6 through 9 were plotted for the pressure-temperature data of this experimental run. Known pressure-temperature curves of carbon dioxide hydrates were additionally plotted.

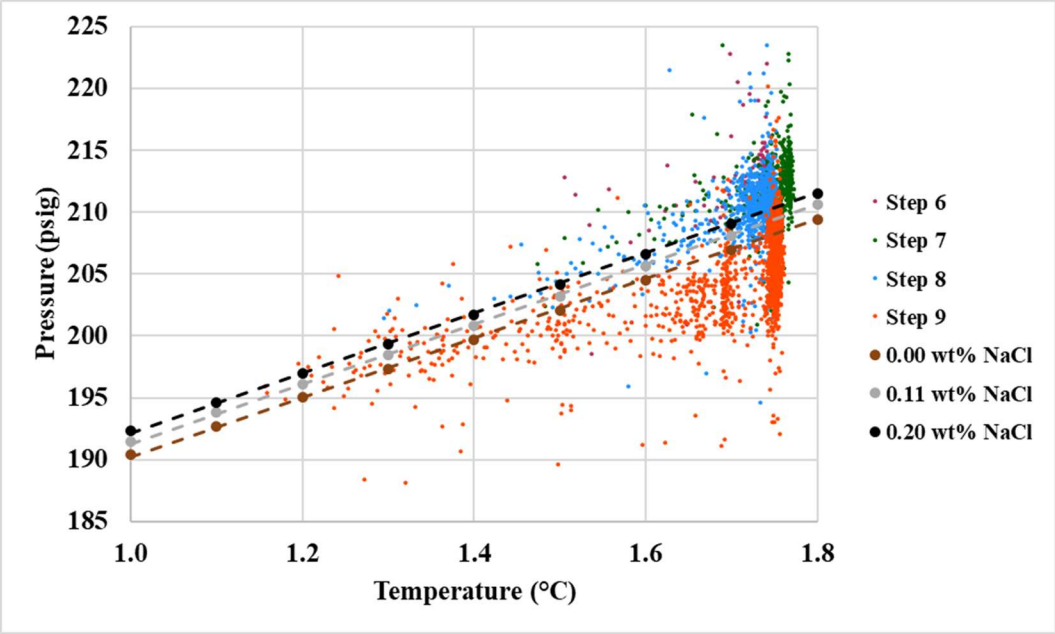

Figure B.5 – Experimental Run 5 Pressure-Temperature Equilibrium

Steps 6 through 9 were plotted for the pressure-temperature data of this experimental run. Known pressure-temperature curves of carbon dioxide hydrates were additionally plotted.

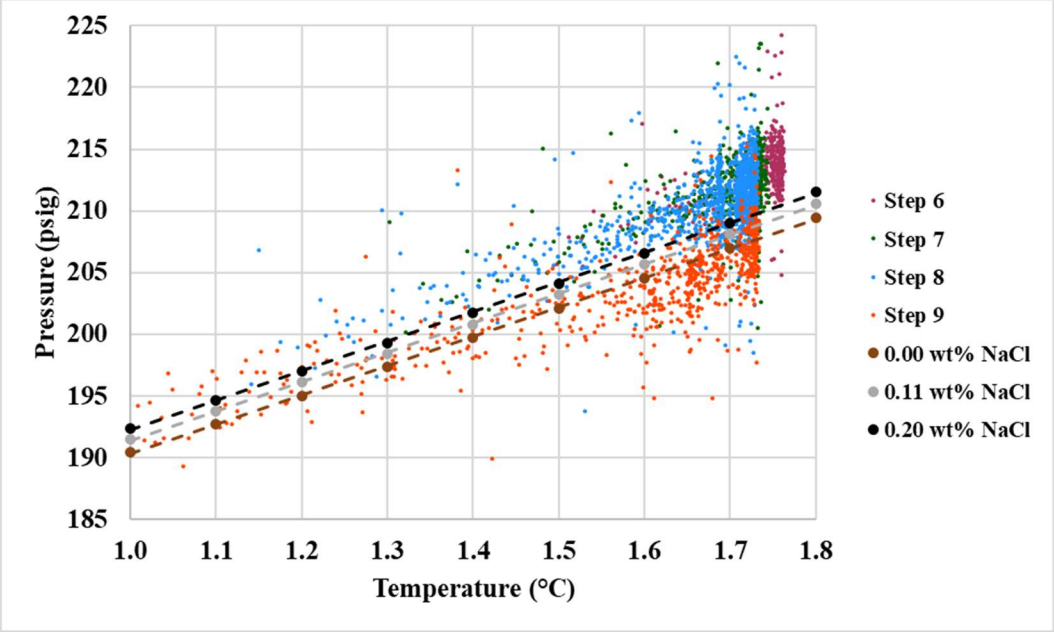

Figure B.6 – Experimental Run 6 Pressure-Temperature Equilibrium

Steps 6 through 9 were plotted for the pressure-temperature data of this experimental run. Known pressure-temperature curves of carbon dioxide hydrates were additionally plotted.

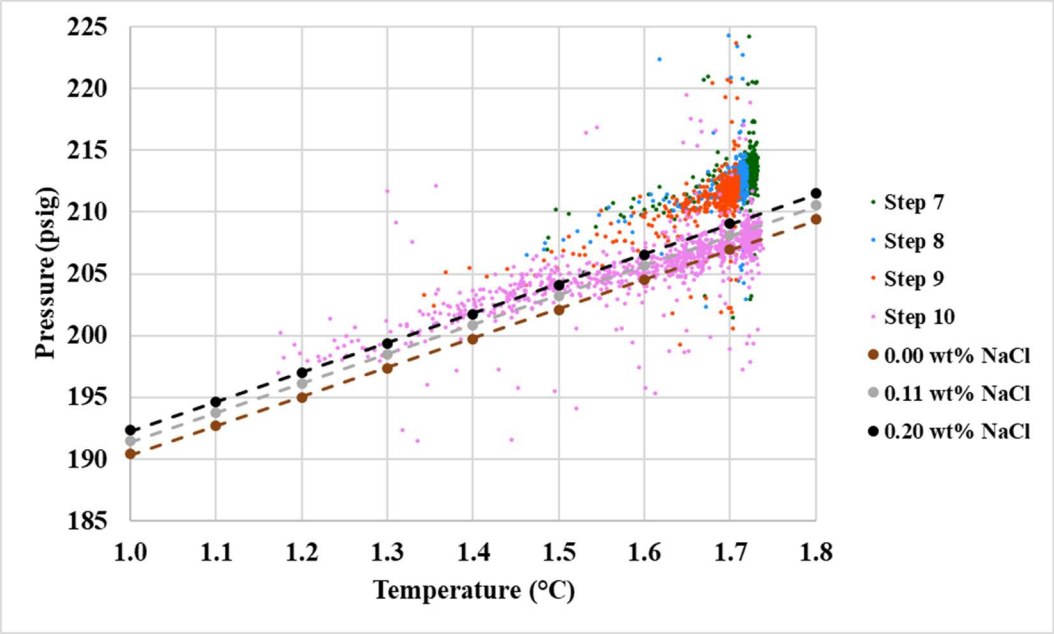

Figure B.7 – Experimental Run 7 Pressure-Temperature Equilibrium

Steps 7 through 10 were plotted for the pressure-temperature data of this experimental run. Known pressure-temperature curves of carbon dioxide hydrates were additionally plotted.

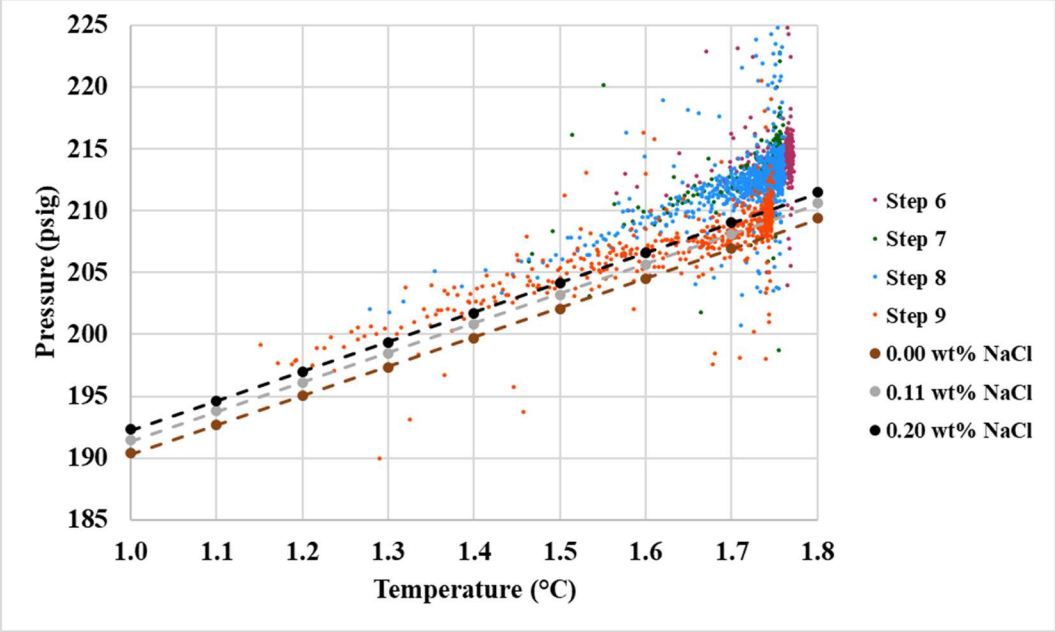

Figure B.8 – Experimental Run 8 Pressure-Temperature Equilibrium

Steps 6 through 9 were plotted for the pressure-temperature data of this experimental run. Known pressure-temperature curves of carbon dioxide hydrates were additionally plotted.

REFERENCES

Abishek, M. P., Patel, J., & Rajan, A. P. (2014). Algae Oil: A Sustainable Renewable Fuel of Future. *Biotechnology Research International*, *2014*, 1–8. DOI: 10.1155/2014/272814

AGAMERICA LENDING. (2017, March 10). Top 10 Produce Crops Grown in the U.S. Retrieved from https://agamerica.com/power-of-10-top-10-produce-crops-in-the-u-s/

Alalwan, H. A., Alminshid, A. H., & Aljaafari, H. A. S. (2019). Promising evolution of biofuel generations. Subject review. *Renewable Energy Focus*, *28*, 127–139. DOI: 10.1016/j.ref.2018.12.006

AllAmericanCooker.Com. (n.d.). All American Electric Sterilizer 25X-120V. Retrieved from http://www.allamericancooker.com/allamerican25xsterilizer.htm

ALL ABOUT algae.com. (2012, February 6). Biofuels: History, Demonstrations, End-products, Production Process, Costs FAQ. Retrieved from http://allaboutalgae.com/faq-history/

De-Bashan, L. E., Moreno, M., Hernandez, J.-P., & Bashan, Y. (2002). Removal of ammonium and phosphorus ions from synthetic wastewater by the microalgae Chlorella vulgaris coimmobilized in alginate beads with the microalgae growth-promoting bacterium Azospirillum brasilense. *Water Research*, *36*(12), 2941–2948. DOI: 10.1016/s0043-1354(01)00522-x

Department of the Interior, U.S. Geological Survey. (2017, October 20). Exploring Gas Hydrates as a Future Energy Source. Retrieved from https://www.usgs.gov/news/exploring-gas-hydrates-a-future-energy-source

DuByne, D. (2012, November 23). Algae. Retrieved from http://www.oilseedcrops.org/algae/

Enerdata. (2019, July 9). Total Energy Consumption by Country. Retrieved from https://yearbook.enerdata.net/total-energy/world-consumption-statistics.html

Fakharian, H., Ganji, H., & Naderifar, A. (2017). Desalination of high salinity produced water using natural gas hydrate. Journal of the Taiwan Institute of Chemical Engineers, 72, 157–162. DOI: 10.1016/j.jtice.2017.01.025

Farm-Energy. (2019, April 3). Algae for Biofuel Production. Retrieved from https://farm-energy.extension.org/algae-for-biofuel-production/

Food and Agriculture Organization of the United Nations. (n.d.). 2.3. Algal production. Retrieved from http://www.fao.org/3/w3732e/w3732e06.htm

Gaarder, C., & Englezos, P. (1995). The use of clathrate hydrates for the concentration of mechanical pulp mill effluents. Nordic Pulp & Paper Research Journal, 10(2), 110–113. DOI: 10.3183/npprj-1995-10-02-p110-113

Guccione, A., Biondi, N., Sampietro, G., Rodolfi, L., Bassi, N., & Tredici, M. R. (2014). Chlorella for protein and biofuels: from strain selection to outdoor cultivation in a Green Wall Panel photobioreactor. *Biotechnology for Biofuels*, *7*(1), 84. DOI: 10.1186/1754-6834-7-84

Hanagata, N., Takeuchi, T., Fukuju, Y., Barnes, D. J., & Karube, I. (1992). Tolerance of microalgae to high CO2 and high temperature. Phytochemistry, 31(10), 3345–3348. DOI: 10.1016/0031-9422(92)83682-o

Heriot-Watt Institute of Petroleum Engineering. (2018). What are Gas Hydrates? Retrieved from https://www.pet.hw.ac.uk/research/hydrate/hydrates_what.cfm@hy=what.html

Kang, S.-P., & Lee, H. (2000). Recovery of CO2 from Flue Gas Using Gas Hydrate: Thermodynamic Verification through Phase Equilibrium Measurements. Environmental Science & Technology, 34(20), 4397–4400. DOI: 10.1021/es0011481

Knothe, G. (2010). Biodiesel and renewable diesel: A comparison. *Progress in Energy and Combustion Science*, *36*(3), 364–373. DOI: 10.1016/j.pecs.2009.11.004

Mimachi, H., Takeya, S., Yoneyama, A., Hyodo, K., Takeda, T., Gotoh, Y., & Murayama, T. (2014). Natural gas storage and transportation within gas hydrate of smaller particle: Size dependence of self-preservation phenomenon of natural gas hydrate. Chemical Engineering Science, 118, 208–213. DOI: 10.1016/j.ces.2014.07.050

National Biodiesel Board. (2008, June 1). Feedstocks - The Future of Biodiesel. Retrieved from https://www.biodieselsustainability.com/feedstocks/

National Center for Marine Algae and Microbiota. (n.d.). Algal Media Compositions. Retrieved from https://ncma.bigelow.org/cms/page/view/page_id/19/

National Oceanic and Atmospheric Adminstration. (2020, April 6). Global Monitoring Laboratory - Global Greenhouse Gas Reference Network. Retrieved from https://www.esrl.noaa.gov/gmd/ccgg/trends/global.html

Newman, S. (2020, January 27). How Algae Biodiesel Works. Retrieved from https://science.howstuffworks.com/environmental/green-science/algae-biodiesel2.htm

Ritchie, H. (2017, August 7). How long before we run out of fossil fuels? Retrieved from https://ourworldindata.org/how-long-before-we-run-out-of-fossil-fuels

Salih, F. M. (2011). Microalgae Tolerance to High Concentrations of Carbon Dioxide: A Review. Journal of Environmental Protection, 2, 648–654. DOI: 10.4236/jep.2011.25074

Sharma, K. K., Garg, S., Li, Y., Malekizadeh, A., & Schenk, P. M. (2013). Critical analysis of current Microalgae dewatering techniques. Biofuels, 4(4), 397–407. DOI: 10.4155/bfs.13.25

Slade, R., & Bauen, A. (2013). Micro-algae cultivation for biofuels: Cost, energy balance, environmental impacts and future prospects. Biomass and Bioenergy, 53, 29–38. DOI: 10.1016/j.biombioe.2012.12.019

Sloan, E. D., & Koh, C. A. (2008). Clathrate Hydrates of Natural Gases (3rd ed.). Boca Raton, FL: CRC Press.

Soomro, R. R., Ndikubwimana, T., Zeng, X., Lu, Y., Lin, L., & Danquah, M. K. (2016). Development of a Two-Stage Microalgae Dewatering Process – A Life Cycle Assessment Approach. Frontiers in Plant Science, 7(113). DOI: 10.3389/fpls.2016.00113

Sung, K.-D., Lee, J.-S., Shin, C.-S., Park, S.-C., & Choi, M.-J. (1999). CO2 fixation by Chlorella sp. KR-1 and its cultural characteristics. Bioresource Technology, 68(3), 269–273. DOI: 10.1016/s0960-8524(98)00152-7

Tan, X. B., Lam, M. K., Uemura, Y., Lim, J. W., Wong, C. Y., & Lee, K. T. (2018). Cultivation of microalgae for biodiesel production: A review on upstream and downstream processing. Chinese Journal of Chemical Engineering, 26(1), 17–30. DOI: 10.1016/j.cjche.2017.08.010

The University of Texas at Austin. (n.d.). Bristol Medium Composition. Retrieved from http://web.biosci.utexas.edu/utex/Media PDF/bristol-medium.pdf

U.S. Department of Energy. (2018, March 30). Biodiesel Blends. Retrieved from https://afdc.energy.gov/fuels/biodiesel_blends.html

U.S. Energy Information Administration. (2017, September 14). EIA projects 28% increase in world energy use by 2040. Retrieved from https://www.eia.gov/todayinenergy/detail.php?id=32912

U.S. Energy Information Administration. (2019, May 14). How much ethanol is in gasoline, and how does it affect fuel economy? Retrieved from https://www.eia.gov/tools/faqs/faq.php?id=27&t=10

U.S. Environmental Protection Agency. (2010, April). National Renewable Fuel Standard Program - Overview [PowerPoint Slides]. Retrieved from https://www.epa.gov/sites/production/files/2015-09/documents/rfs2-workshop-overview.pdf

U.S. Environmental Protection Agency. (2019, December 19). Renewable Fuel Annual Standards. Retrieved from https://www.epa.gov/renewable-fuel-standard-program/renewable-fuel-annual-standards

UTEX Industries. (n.d.)a. Proteose Medium. Retrieved from https://utex.org/products/proteose-medium?variant=30991748169818

UTEX Industries. (n.d.)b. UTEX 2714 Chlorella vulgaris. Retrieved from https://utex.org/products/utex-2714?variant=30992248602714

Waters. (n.d.). Supercritical Fluid Extraction (SFE) Systems. Retrieved from https://www.waters.com/waters/en_US/Supercritical-Fluid-Extraction-(SFE)-Systems/nav.htm?cid=10146521&locale=en_US

Wesoff, E. (2017, April 19). Hard Lessons From the Great Algae Biofuel Bubble. Retrieved from https://www.greentechmedia.com/articles/read/lessons-from-the-great-algae-biofuel-bubble

Wu, X., Ruan, R., Du, Z., & Liu, Y. (2012). Current Status and Prospects of Biodiesel Production from Microalgae. Energies, 5(8), 2667–2682. DOI: 10.3390/en5082667

Wu, B., Horvat, K., Mahajan, D., Chai, X., Yang, D., & Dai, X. (2018). Free-conditioning dewatering of sewage sludge through in situ propane hydrate formation. Water Research, (145), 464–472. DOI: 10.1016/j.watres.2018.08.057

Yeh, K.-L., & Chang, J.-S. (2012). Effects of cultivation conditions and media composition on cell growth and lipid productivity of indigenous microalga Chlorella vulgaris ESP-31. *Bioresource Technology*, *105*, 120–127. DOI: 10.1016/j.biortech.2011.11.103